TELECAT project

New Teleseismic Catalogue for NOA – Bridging the gap

Report # 1

Preliminary results using data from 2019

Fevronia Gkika (1) and Jens Havskov (2)

(1) Institute of Geodynamics, National Observatory of Athens, Greece
(2) Department of Geoscience, University of Bergen, Norway

Emails:gkika@noa.gr , Jens.Havskov@uib.no

01/11/2023

Introduction

For the last 20 years, there has been an absence of organized efforts to analyze teleseismic occurrences documented by Greece's seismic stations. Recognizing the significance of processing and documenting these teleseismic events, a decision was made to seek funding for a project focused on reviewing the most crucial events between 2012 and 2021. This proposal was granted approval on January 1, 2023, in the form of an internal scholarship awarded to Dr. Fevronia Gkika, research scientist C. The undertaking is being carried out at the Geodynamic Institute of the National Observatory of Athens (GI/NOA) in partnership with Bergen University.

The seismic data will be used for different kinds of analysis like earthquake magnitude statistics and comparing hypocenters to the global solutions. This way magnitude calculations and location ability will be evaluated and any network characteristic either picking phase accuracy will be revealed. Since processing 10 years of data requires a significant effort, this work started with a pilot study using a sample data set for the year 2019. During this initial pilot study, various combinations of station selections and parameter settings are being tested. The aim is to find the best setup that will work optimally for the larger data set. The concept involves choosing events using the ISC catalog, read seismic phases and determine four different magnitude types: body wave magnitudes MB and Mb and surface wave magnitudes MS and Ms. During this preliminary study, the outcomes will be compared to the solutions provided by the ISC catalog. The process and the findings will be detailed in the upcoming sections.

Station selection from the Hellenic Unified Seismic Network

Hellenic Unified Seismic Network (HUSN) is an extensive seismic network comprising almost 150 stations nationwide which is in continuous operation with real-time data transmission. Two-thirds of the stations are equipped with triaxial broadband seismometers, while the remaining one-third use triaxial short-period seismometers. Since this is a large dataset, even for this initial study of the year 2019, a subset of stations and channels were selected for processing. The selection was based on sensor type, operational availability and stability in this time period, geographical distribution and known ambient noise characteristics. More specifically, only the best broadband sensors from HUSN were used like Streckeisen STS2-120s, Nanometrics Trillium 120s and Guralp 3ESPC 60-100s. A total of 103 stations has been selected for the analysis of teleseismic events, as depicted in Figure 1.

*Figure 1: Station distribution of the **Hellenic Unified Seismic Network** (HUSN) used in this study. The orange triangles represent broadband stations where only data from Z component are utilized, while the yellow triangles represent stations that we use data from all three components.*

Given the substantial volume of data, waveforms from the Z components are exclusively employed for the majority of stations, with a focus on broadband stations. To precisely establish the onset times of S-type phases, a subset of 18 stations with three components is also examined, Figure 2. These stations are HL.ARG, HL.APE, HL.ATH, HL.GVD, HL.IACM, HL.IDI, HL.IMMV, HL.ITM, HL.KARP, HL.KLV, HL.KEK, HL.KTHA, HL.PRK, HL.SMG, HL.THERA, HL.THL, HL.VLS and HL.ZKR. These stations were chosen for their strong attributes and consistent operational performance mostly equipped with STS2-120s and Trillium-120s. Figure 2 provides an example of traces from a single station.

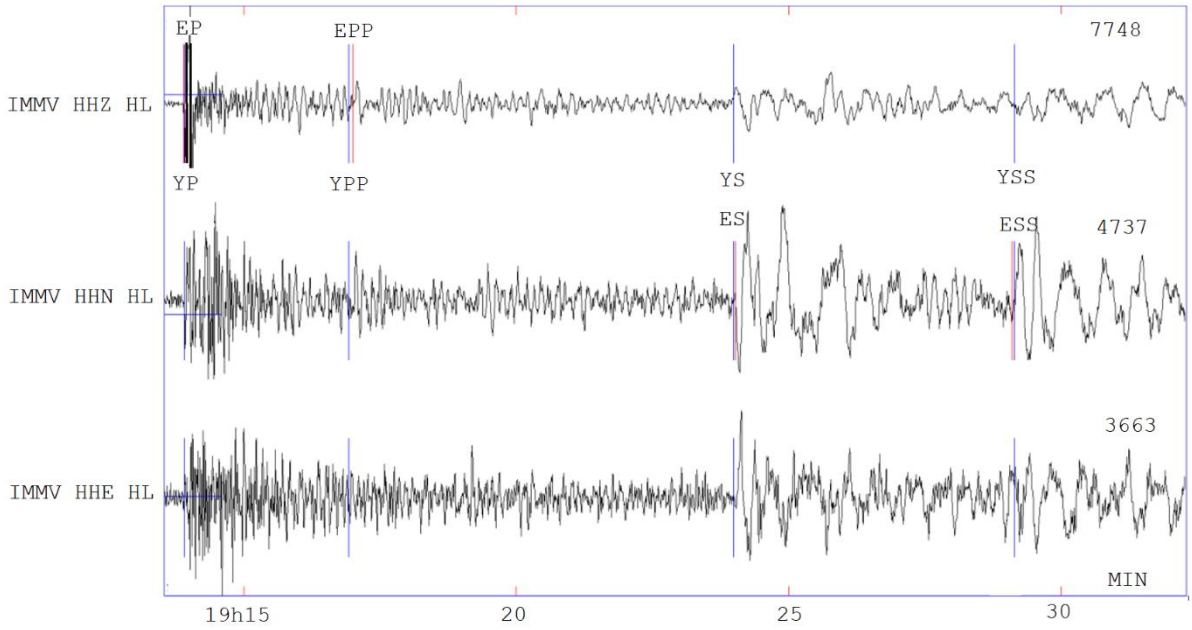

Figure 2: Example of S type phases on a 3 component station HL.IMMV. Manually picked phases are marked in red and the theoretical arrival times are marked in blue. The theoretical phases are distinguished by the prefix "Y" in their names. The numbers to the right are maximum amplitudes in counts. The blue line at the start of the trace indicates the DC level.

Event selection

Several tests were conducted to identify events in the ISC catalog that would likely be detected by a majority of stations as global events. It turned out that selecting events with ISC Mb ≥ 6.0 was a reasonable choice. The option of using all types of magnitudes from all agencies, as long as they are greater than or equal to 6, was dismissed due to the inclusion of unreliable magnitudes by some agencies resulting in the selection of events with magnitudes that were too small. ISC receives data from 150 different agencies and reports 39 types of magnitude, but only calculates Mb and Ms (Havskov and Lieser 2021). In order to get the most reliable hypocenters, only events with hypocenters calculated by ISC were selected and only if this hypocenter was designated as the prime hypocenter by ISC. The output from the ISC search engine is hypocenter and magnitudes in ISF format (extension of IMS format). For the year 2019, there were 76 events fulfilling these criteria, Figure 3.

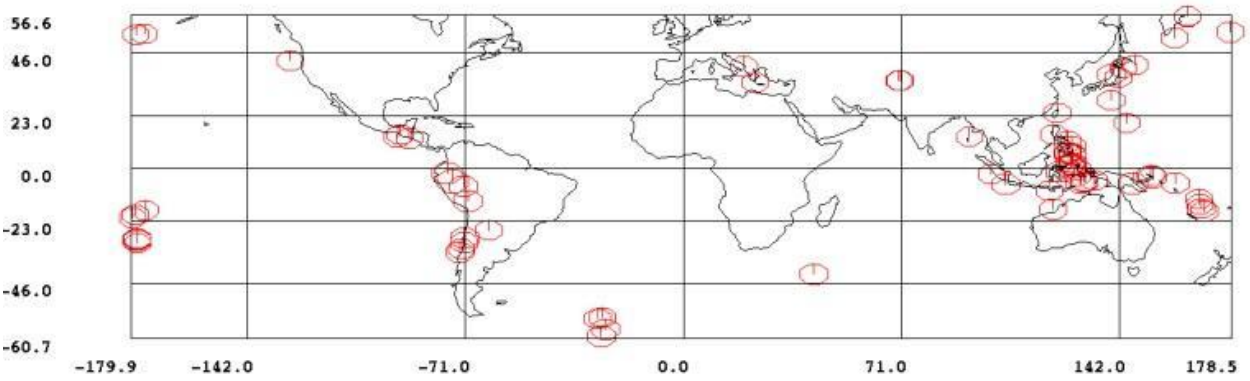

Figure 3: A total of 76 events from ISC for the year 2019 with magnitude Mb≥6.

Processing

The processing involves reading phases and amplitudes and relocating in order to check the residuals. Since, the selected events typically have more than 1000 phases picked, relocating the events together with the existing phases would pose challenges in distinguishing residuals from Greek stations and demand a significant amount of time, so no phases were selected from ISC for the relocation process. Instead, the idea is to fix the hypocenter to the ISC solution, pick the phases and amplitudes from Greek stations and then relocate and acquire the residuals for this ISC solution. Fixing the hypocenter is motivated by the potential difficulty in obtaining a dependable hypocenter for distant events using solely Greek stations. Consequently, it would be also difficult to judge if the residuals for HUSN stations are reasonable.

Software

GI/NOA employs the SeisComP *scolv* software 2018 version for the routine seismicity analysis, by Helmholtz-Centre Potsdam - GFZ German Research Centre for Geosciences and gempa GmbH (2008). In principle *scolv* can serve as the processing tool, but it requires injecting the ISC parametric data into the Seiscomp SQL database and setting up all the station metadata. Furthermore, *scolv* software does not support the option of fixing the hypocenter. Lastly, the process of loading approximately 2 hours of continuous data is characterized by a notably slow speed. Hence, the initial processing task was performed by SEISAN software (Havskov et al. 2020).

Each ISF file from ISC was converted to the Nordic format used by SEISAN and inserted in a SEISAN database called ISC. The data can now be plotted directly from the archive. Nevertheless, similar to SeisComP, this approach also exhibits a relatively slow processing speed so the event waveform files corresponding to the ISC events were extracted from the archive using the SEISAN program get_arc. The extracted data comprises waveforms spanning a duration of 3 minutes before the origin time, extending up to 2 hours after. Collected waveform data are placed in the ISC database in the WAV directory. The

SEISAN database then consists of single files with hypocenter, phases, amplitude readings (S-file) and corresponding waveform files.

S-files include a header that contains a description of the teleseismic event (origin time, epicenter, depth, magnitude, etc) and a following line gives a link to the waveform file in the WAV directory (relative path SEISAN/WAV). An example of an event S-file before processing starts, is shown below.

```
2019 0201 1614 12.4 DQ 14.771 -92.279 78.1FFISC999 2.3 6.1bISC         6.1bISC
GAP= 24   ISC 0.250       3.4     3.4  1.9
2019 0201 1614 12.4 DQ 14.771 -92.279 78.1FFISC999 2.3 6.1bISC         6.1bISC
LOCALITY:    614610371 Southern Sumatera
2019-02-01-1615-11M.NSN___107
STAT COM NTLO IPHASE   W HHMM SS.SSS   PAR1  PAR2 AGA OPE  AIN  RES W  DIS CAZ
```

Example 1: On the Header line (first line) the double FF indicates fixed hypocenter and epicenter of the ISC solution. LOCALITY describes the area of the earthquake (4th line) and the line below has the name of the waveform file (5th line) linked with this event (identified by type 6 at column 80), which is located in the WAV directory. Duplicated ISC solution is on the 3rd line in order to retain the original ISC location and magnitude.

Picking Phases and Location

Analysis of teleseismic events begins with the picking of P and S phases without any type characterization assuming them to be first arrivals. This is done to avoid problems with phase names in locations and thus just refers to the first phase of P or S type. Most location programs will then automatically reinterpret the first arrival P and S phases with the correct name characterization (e.g. Pdif, P, PKP, S, SKS). Phase picking is done only if phases can be clearly seen and S-type phases are picked normally only from horizontal components. Although filtering is available in SEISAN, phase picking is done with no filter. Applying a filter causes time shifting by delaying the onset (filter passes one way). It is possible to let the filter pass both ways to avoid time shift but this broadens the signal. In some cases, it is not possible to see the phase without a filter and we have chosen not to use the data in this case.

Using the fixed depth and epicenter for the events from ISC solutions, theoretical arrival times can be calculated and plotted for a set of different phase types as defined in the file IASP.DEF file (relative path SEISAN/DAT/IASP.DEF). Not all possible phases are used since this would clutter up the plots and many of the rarer phases are seldom seen. We selected the following phases: P, Pdif, PP, PKP, pP, pPKP, PcP, S, SS, SKS. Plotting the theoretical arrival times is very helpful for teleseismic analyses.

After picking P and S, extra phases are picked with phase type characterizations such as pP, PP, SS. This extra info improves the hypocenter parameters accuracy and enriches the catalogue with valuable information.

Amplitudes for magnitudes are also picked, see later section.

Phase names follow the recommendations of the IASPEI Commission on Seismological Observation and Interpretation (Storchak et al., 2003, Storchak et al., 2011, http://www.isc.ac.uk/standards/phases/).

In the following Figure 4 and Figure 5, examples of two different teleseismic events are presented. Figure 4, shows traces with no filter of a shallow teleseismic event on 22/01/2019 19:01:44 of magnitude Mb 6.4 (ISC Prime solution). It is located at Aru Islands with a distance of 8809 Km from the closest station (ZKR) of the Greek network. This event is well recorded on different stations of HUSN and phase arrivals plus amplitude measurements are clear.

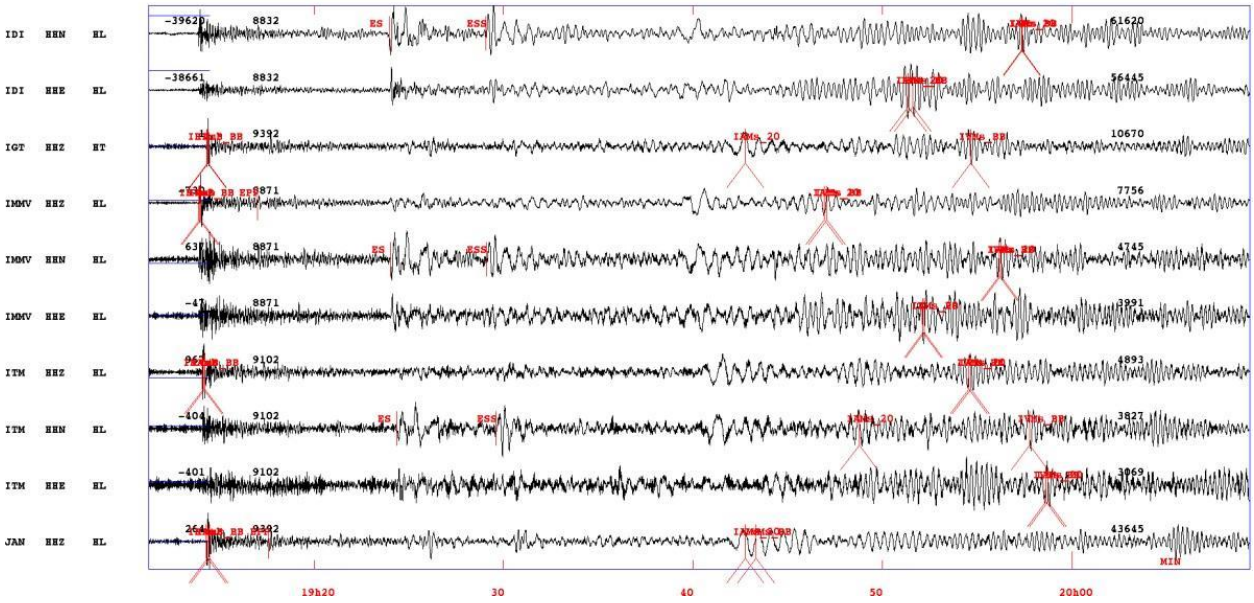

Figure 4: Manually picked phases and amplitudes for event at 22/01/2019 19:01:44, Mb is 6.4 ISC, Aru Islands. The signal has not been filtered.

A deep event (h= 584 km) with low signal to noise ratio, is presented in Figure 5. It is located at Northern Molucca Sea with a distance from the closest station (KEK) 10716 Km of the Greek network.

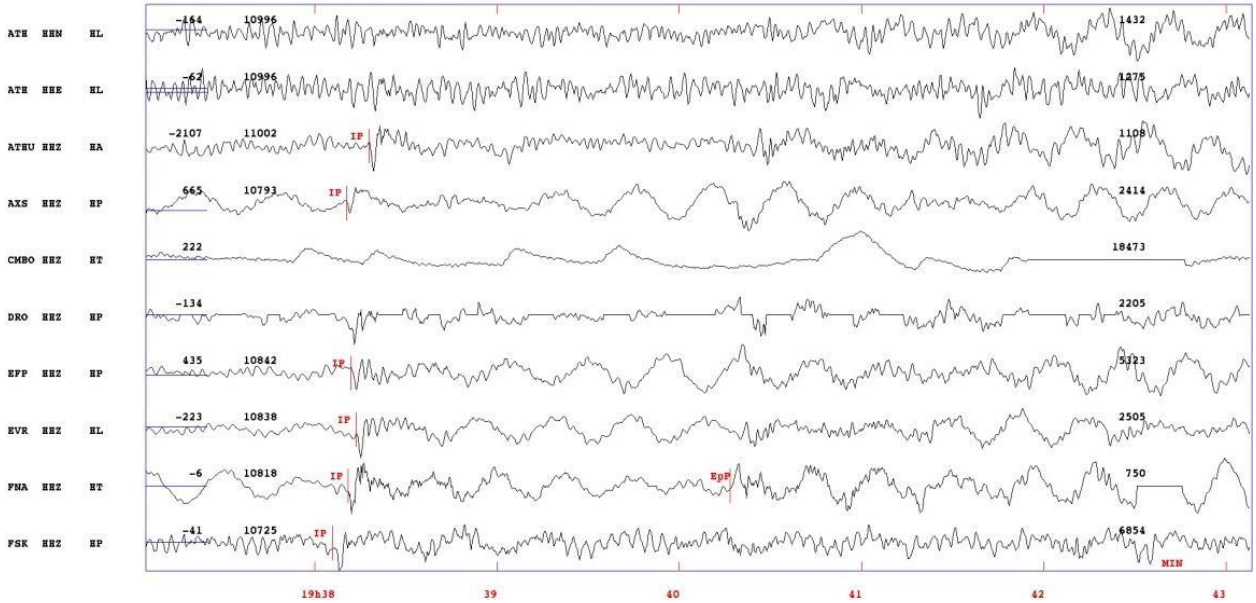

Figure 5: A deep event (h=584 km) on the 05/01/2019 19:25:40 with magnitude Mb 6.3 ISC. The traces are unfiltered.

Few phases can be picked since it is not well recorded in many stations. The P onsets could only be identified with a high zoom around the phases.

Earthquake source parameters calculation is done with the **hypocenter** program (part of SEISAN) that locates teleseismic events. It is a modified version of HYPOCENTER (Lienert et al., 1986; Lienert, 1991; Lienert and Havskov, 1995). It should be noted that SEISAN uses IASP91 (Kennett and Engdahl, 1991) earth model while ISC uses Ak135 (Kennett et al., 1995) so there will be small differences in the travel times calculated by the 2 models.

When phase picking is complete a first location is done with fixed depth and epicenter. For this location, the travel time rms are usually similar to or lower than ISC rms depending on the type and number of phases. With a P residual < 1 sec and only few S phases, residuals are close to 1 sec, max 1-1.5. When more phases are added (SKS, PP, SS etc) rms becomes higher but always similar or smaller than ISC. This is what we should expect since we use much less phases than ISC. Stations that had a consistent time error were not used (e.g. HL.VLY constant high residuals >> 3 sec) and are weighted out, however, their residuals are calculated. In addition, stations with bad signal to noise ratio (e.g. HT.CMBO, occasionally HP.DRO) or a temporary malfunction (e.g. HL.IACM) were not used. Doing the processing in this way will ensure that we do a good quality check of the arrival times. Some observations were extracted from the analyses of the 2019 dataset. Residuals of Pdif, P, PKP and pP are usually around 1 sec max 1.5 sec, S and SKS are up to 2 sec most of the time and sometimes up to 5-6 sec maximum, so we would accept them up to 3 or even 4 sec. Residuals of PP are around 2 sec and SS exhibits always higher residuals around 3-6 sec.

When picking is finished and the quality of the arrival times has been checked, the event is relocated in two stages (fixed depth and unfixed epicenter, unfixed depth and unfixed epicenter) in order to see how well the event can be located using only phases from the Greek stations. An S-File example of an event located with only Greek stations with an unfixed solution, is the following:

```
2019 0122 0510 05.0 D  -7.327 120.011 6.90  NOA 64 1.1 6.3sNOA 6.3SNOA 6.0bISC
GAP=353   NOA  2.94     139.5   110.0  7.5  0.1490E+05  0.1332E+03  0.2380E+03
2019 0122 0510 05.2 D -10.288 119.130 34.7  ISC999 2.2 6.0bISC 6.4sISC 6.0bISC
GAP= 30   ISC 0.340       3.6     3.6  1.4
LOCALITY:    614617830 Prince Edward Islands region
2019-01-22-0511-04M.NSN___106
STAT COM NTLO IPHASE   W HHMM SS.SSS   PAR1  PAR2 AGA OPE  AIN  RES W  DIS CAZ
KSL  HHZ HL    IAMs_20   0608 58.43015762.5  20.5 NOA fd       0.13  10532 306
KSL  HHZ HL    IVMs_BB   0609 05.290 4815.3  17.7 NOA fd       0.13  10532 306
ARG  HHZ HL   IP         0523 32.050              NOA fd  14.0 0.021010663 306
ARG  HHE HL   ES         0534 10.070              NOA fd   9.0 1.771010663 306
ARG  HHZ HL    IVMs_BB   0610 48.060 3095.7  24.1 NOA fd      -0.06  10663 306
ARG  HHZ HL    IAMs_20   0610 54.640 9972.5  21.4 NOA fd      -0.08  10663 306
SMG  HHZ HL   IP         0523 37.770              NOA fd  14.0 0.571010790 307
SMG  HHZ HL   EPP        0527 32.610              NOA fd  24.0 0.371010790 307
SMG  HHE HL   ES         0534 15.650              NOA fd   9.0 1.311010790 307
SMG  HHZ HL    IVMs_BB   0611 11.600 3927.9  22.4 NOA fd       0.05  10790 307
```

```
SMG  HHZ HL    IAMs_20   0611 15.44013958.9  21.4 NOA fd       0.07  10790 307
ZKR  HHZ HL   EP         0523 38.150              NOA fd  14.0-0.511010826 304
ZKR  HHZ HL   EPP        0527 36.910              NOA fd  24.0 2.181010826 304
ZKR  HHZ HL    IVMs_BB   0611 17.340 5610.0  21.4 NOA fd       0.21  10826 304
ZKR  HHZ HL    IAMs_20   0611 20.95019922.1  23.0 NOA fd       0.20  10826 304
```

The first line of the header shows the solution derived by NOA data and below the ISC solution as kept for comparison purposes on the 3rd line. Information of the stations used, amplitude measurements and phase readings with all their accompanied information are described in this file.

Among the 76 events of 2019, six events could not be used due to low signal to noise ratio despite these events having a large magnitude ($6 \leq Mb \leq 6.3$), see Appendix I and Figure 6. The events are low frequency (can only be seen with a filter 0.01-0.1 Hz) and most of them are located at distances > 11000 Km, in the Vanuatu area (one deep event), two in Banda Sea, one in the South Pacific and the rest in South America. In addition, two events were rejected as local, so they had already been processed by NOA.

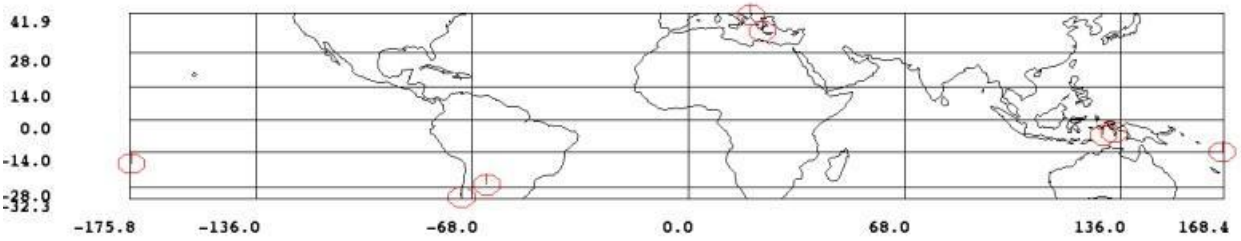

Figure 6: Events not processed. Two events are Local and six are teleseismic low frequency events of magnitude Mb ≤ 6 with a low signal to noise ratio.

Considering the minimum number of stations needed to obtain an unfixed solution: In practice we have located satisfactory with just 7 -10 stations (e.g. HL.THL, HL.KLV, HP.GUR, HL.IDI, HL.KEK, HL.ZKR, HL.KZN etc.) distributed all over the territory of Greece so this is the minimum number of stations to obtain a satisfactory solution. Distance and probably the region is affecting the minimum number of stations that is needed and of course, how many different types of phase readings (P, S) available. The most important in the locations after picking the first arrivals is to include, when possible, well identified later arriving phases. In terms of depth determination at teleseismic distances, except S-type phases, depth phases such as pP, pPKP can further improve the hypocenter solution. So as many quality phases as possible were read. In the following Figure 7, is presented the comparison between the teleseismic events as located by HUSN stations only (unfixed depth and unfixed epicenter) and the ISC solutions.

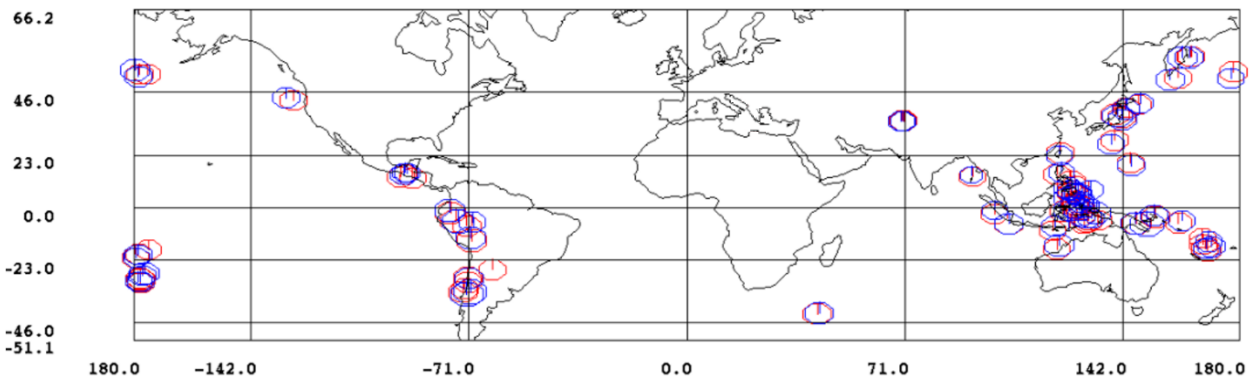

Figure 7: Teleseismic events of 2019 with magnitude Mb ≥ 6 that were located using HUSN stations (Blue, unfixed solutions) in comparison with the ISC solutions (red).

It can be seen that the locations with the HUSN stations in general agree with the ISC locations except for a few events that deviate by a few degrees. These are usually events from Vanuatu, Papua and South Pacific areas with deep core phases arriving Pdif, PKPdf, pPKPdf. Independently of the number of stations used, for these events, a common observation is that the residuals for the fixed solution is usually high leading to an unfixed solution that is deviating more in comparison with the ISC solution. More specific these events are: 14/05/2019 surface event Papua, 31/07/2019 deep event Vanuatu, 06/08/2019 deep event Vanuatu, 21/10/2019 deep event Vanuatu and 08/11/2019 deep event South Pacific (Appendix I).

Table 1, shows a comparison of hypocentral parameters of ISC and HUSN when the HUSN solution is unfixed (depth and epicenter).

Table 1: Comparing the average hypocentral parameters between ISC and HUSN locations using unfixed hypocenters. Coordinate differences are expressed in degrees and Depth in Km.

	Origin time	RMS	Lat	Lon	Depth
Average diff	1.5	0.6	0.065	-0.324	-9.5
Standard dev	7.9	1.0	1.543	1.853	85.8
Number of values		68		68	68

Locations of the teleseismic events using HUSN stations are quite close to the ISC and any differences are almost negligible considering the distances. Noticeable as expected, is that highest deviations occur in terms of depth especially when dealing with deep events. Unfixing the epicenter but keeping the depth fixed to prime ISC solutions the HUSN data slightly improves in epicenter terms as can be seen from the respective observations between ISC and HUSN solutions (Table 2).

Table 2: Comparing the average hypocentral parameters between ISC and HUSN locations using unfixed epicenter and fixed depth. Coordinate differences are expressed in degrees and Depth in Km.

	Origin time	RMS	Lat	Lon	Depth
Average diff	1.4	0.7	0.016	-0.312	0.0
Standard dev	5.3	0.4	1.329	1.784	0.0
Number of values		68		68	68

It should be noted that the purpose of this study is not to locate global events and we do not expect to be able to do so accurately. However, comparing the location gives an idea of how well it can be done and also gives feedback on the accuracy of the phase picks.

Magnitudes

One purpose of this study is to compare magnitudes calculated by NOA and the prime magnitudes calculated by ISC. ISC only calculates body wave magnitude Mb and surface wave magnitude Ms. Both magnitudes are based mainly on the relatively narrow WWSSN standard seismograph response. However, in recent years, these magnitudes have also been calculated using a wider response, the so-called broadband body and surface wave magnitudes, respectively MB and MS. These magnitudes will also be calculated in order to investigate the differences with Mb and Ms. For detailed definitions, see the latest IASPEI standards, by Bormann and Dewey, 2014:

Magnitude Mb is a derivative of MB definition by Gutemberg (1945 a,b, 1956) and is calculated from the maximum amplitude in the P-wave train. It is defined as:

$$Mb = \log(A/T) + Q(\Delta,h) \quad (1)$$

where A is the maximum amplitude in nm or μm (depending on which Q-function is used), T the period and Q the attenuation function as a function of epicentral distance Δ and hypocentral depth h. It is recommended by IASPEI to use the original attenuation functions for P waves (Gutemberg and Richter 1956), which are been used nowadays by the ISC and USGS.

The magnitude relation for broadband MB is in agreement with the original definition by Gutemberg and Richter (1956), which used a wider response than used for Mb. It is defined as:

$$MB = \log(Vmax/2\pi) + Q(\Delta, h) - 3.0 \quad (2)$$

where Vmax is maximum ground velocity in nm/s recorded on a broad band sensor proportional to velocity and Q is the correction function mentioned above. Body wave magnitudes Mb and MB have no depth restrictions. Amplitude measurements are restricted only in the period range. The Mb is calculated in the period range of 0.2-3 sec and MB in the period range of 0.2-30 sec. As a result of the short period range on measurements of Mb, it saturates around magnitude 7 while MB saturates at around magnitude 8. Both magnitudes are calculated in the distances 20°–100°.

Surface wave magnitude was introduced by Gutemberg (1945), is based on the measurements of surface waves amplitudes using the vertical component and generated by shallow earthquakes < 60 Km, defined by the Moskow – Prague formula:

$$Ms = \log (A/T)max + 1.66 * \log\Delta + 3.3 \quad (3)$$

where A is amplitude in μm, T period in sec, and Δ distance in degrees from the epicenter (Karnic et al. 1962, Vanek et al. 1962 , IASPEI 2013). Ms is measured in the distance range 20° -160°.

The Ms magnitude, although depth limited, has the advantage that it can be used for magnitude calculations of earthquakes at a larger distance range than Mb.

Since the early 60s and after the introduction of WWSSN, in most agencies, Ms calculations refers to measurements of surface wave amplitudes applied in a narrow period range between 18 – 22 sec and teleseismic distances 20° – 160°, (Oliver and Murphy, 1971; Peterson and Hutt, 2014, Di Giacomo 2022).

Broadband magnitude MS in contrast with Ms, is used on wider distance ranges between 2◦ to 160◦ and a wider period ranges of 3 to 60 s. The larger period means that, for large events, the magnitude is less affected by the local structure. The smaller period and the smaller distance mean that MB can be used for local and regional events. Thus, it is expected that MB will have a much wider use and applicability and is particularly valuable for large regional events.

All these magnitude types Mb, MB, Ms, MS have been calculated for the available dataset with respect to their restrictions by definition.

Magnitude residuals – station check

In order to check the magnitudes, average station magnitude residuals were calculated for all stations, Appendix II. The residuals are calculated as the difference between the average event magnitude and the station magnitude. The residuals are small for most of the stations used, implying an internal consistency in the measurements. The most deviating stations (average residual ≥ 0.25) are presented in Table 3. The deviating magnitudes are shown in bold. The other magnitude residuals for the same station are also shown.

Table 3: Stations of HUSN with average magnitude residuals higher than 0.25 checked for magnitudes MB, Mb, MS and Ms.

AVERAGE MAGNITUDE RESIDUALS DEVIATING ≥0.25												
Mb				**MB**			**Ms**			**MS**		
STAT	N	AV	SD	N	AV	SD	N	AV	SD	N	AV	SD
IACM	13	**0.47**	0.31	13	0,23	0,22	26	**-0.3**	0.21	34	-0,2	0,22
TETR	26	**0.31**	0.23	28	0,2	0,14	33	0,06	0,1	37	0,04	0,12
THL	23	**0.28**	0.27	23	0,2	0,14	38	0,03	0,11	39	0,03	0,1
HORT	29	**0.27**	0.21	30	0,2	0,09	39	0,06	0,11	39	0,04	0,11
KARP	23	**0,31**	0,28	23	**0,26**	0,21	36	0.00	0,18	34	0,01	0,18
PRMD	10	**0.25**	0.28	10	0,24	0,17	15	0,01	0,07	15	0,02	0,06
ARG	22	0,21	0,19	23	0,14	0,18	36	**-0.28**	0.15	20	**-0.33**	0.16
KNT	30	0.00	0,23	30	0,11	0,16	30	**0.63**	0.14	3	**0,74**	0,08

It is seen that the residuals for Mb and MB have the same sign and likewise for Ms and MS which indicate that the residual is related to the station (structure or technical). On the other hand, the residual for body waves and surface waves do not in general have the same sign indicating that the source of the residual is the structure and therefore not a technical problem.

The deviating stations were further checked. Noise spectra were made to check obvious instrument gain problems; however, a factor of 2 gain error can probably not be seen. It seems that all noise spectra (the following figures) have nearly the same noise level around 0.1-0.3 Hz so comparing the noise level at that frequency band gives an indication of a gain problem. Differences in noise amplitude level for higher or lower frequencies can be caused by instrument problems but most likely by different local noise levels at high frequencies and bad installation at low frequency. The ground motion in terms of velocity was compared to ground motion of the good station KLV. For P-waves, a filter 0.5-3 Hz was used and for surface waves 0.01-0.1 Hz respectively. In some cases, due to instability, a filter 0.03-0.1 Hz was applied instead. KLV is located in

Kalavryta area in Peloponnese, on thick-bedded to unbedded fractured limestone and can be characterized as a hard bedrock site. The station has near zero magnitude residuals (Appendix II) so it therefore represents the average ground amplitude level for the network.

STATIONS CHECK

The intention of this check is to detect probable instrument malfunctioning and, if that is the case, to exclude a station from magnitude calculations. The main purpose in this section is to highlight that the amplitude measurements are made from well operating stations. In this way we can ensure that all magnitude calculations are correct and any magnitude deviation then will be accepted as network characteristic.

Probable stations structural effects will be mentioned briefly. Most of the following referenced stations are located on the so-called seismic bedrock but due to the complex geotectonic setting of Greece there are some structural differences that should be highlighted, Figure 8. Particularly, the stations IACM, KLV, KARP and ARG are located on the forarc of the active subduction across the Hellenic arc. The complex structure of the subducting plate is characterized by an increasing slope from west to east across the southern Hellenic arc. Segmentation and slab tearing has been inferred in the area between Eastern Crete and Karpathos (Bocchini et al. 2018.) Stations TETR, KNT at the northwestern and northern part of Greece are located either in the area where continental collision occurs north of the CTF or in the backarc area of the Hellenic arc.

Morphological differences among stations are observed too. The stations are located either inside basins or at higher altitudes on mountain chains, so depending on the station topographic effects might be considered, too. Due to the absence of station inventory with geological information, the geological setting is described from geological maps, 1:50.000 by IGME (Institute of Geological and Mineral Exploration) and/or site inspection.

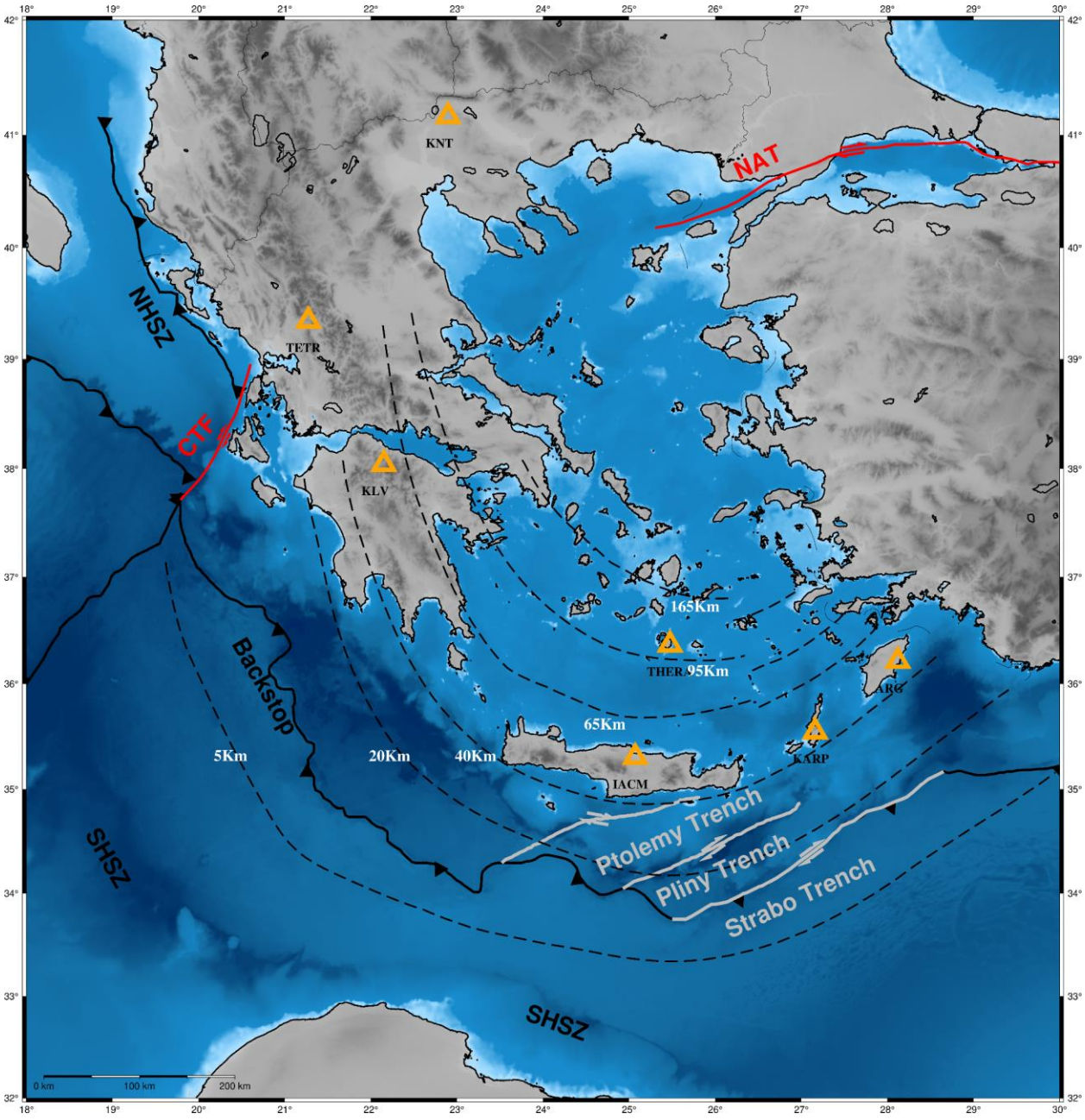

Figure 8: Combined map with the main features of the Hellenic Subduction Zone, the Northern part NHSZ and the Southern SHSZ. The Backstop of the African plate with the Aegean microplate, CTF Cephalonia Transfer Fault, NAT part of the North Anatolian Fault, Ptolemy, Pliny and Strabo offshore trenches southern of Crete, Kreemer C. & Chamot-Rooke N. 2004. Dotted black lines represent the oceanic slab isodepths of 5 Km, 20 Km ,40 Km, 65 Km, 95 Km, 165 Km, Bocchini et al. 2018. Stations ARG, IACM, KARP, KLV, KNT, TETR plus THERA station on Santorini volcanic island.

IACM

The station is located in Heraklion basin Crete and belongs to the HL network. The geological setting in the area of the station are carbonated sediments such as marls, sandy marls, clays, diatomites and

limestones based on the geological map of IGME, Herakleion sheet. It is placed in a good seismic vault but at the edge of the city and within the Neogene basin, as a result, cultural noise is expected to be present. The station shows too high mb and too low Ms. In most of the teleseismic records, the noise obstructs the P arrivals indicated by the low number of Mb, MB observations. The station is characterized with high noise levels especially above 0.5 Hz and below 0.1 Hz, Figure 9. If Mb magnitude is measured at lower periods (0.5-2 sec) around 1 Hz and up, high level of noise occurs and might give misleading magnitude results. However, it results in fewer readings made. The P-wave amplitude is higher than for KLV while the surface wave amplitudes are similar (Figure 10) as also seen in the opposite sign of the residuals for body and surface waves. This indicates that the gain is ok so if it is ensured that the signal to noise ratio is ok, the amplitude values can be used.

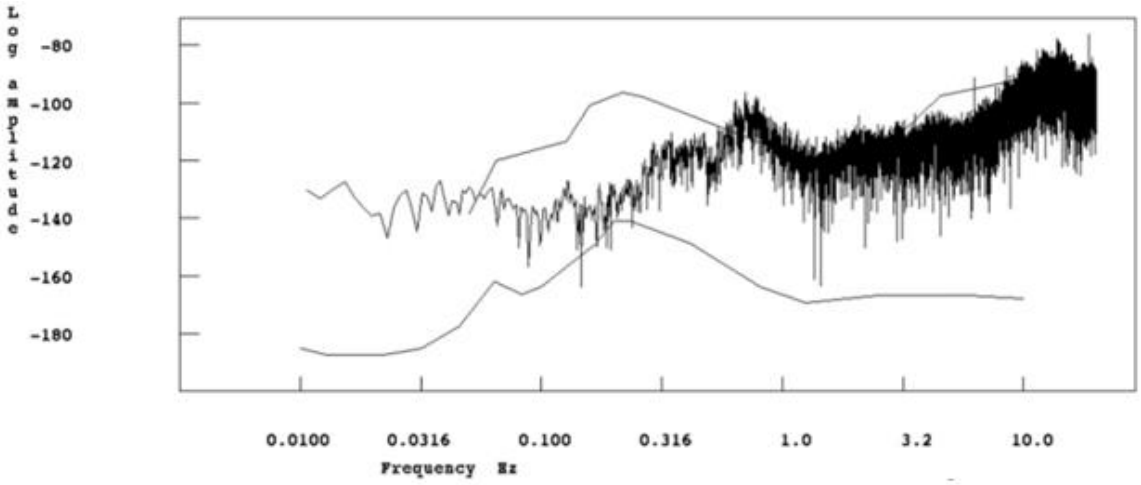

Figure 9: Seismic background noise as acceleration power spectral density in dB relative to (m⁄s^2)^2/Hz . Station IACM, event 22/01/2019 19:01:42. Peterson (1993) curves of the new global high and low noise models are superimposed on the spectrum.

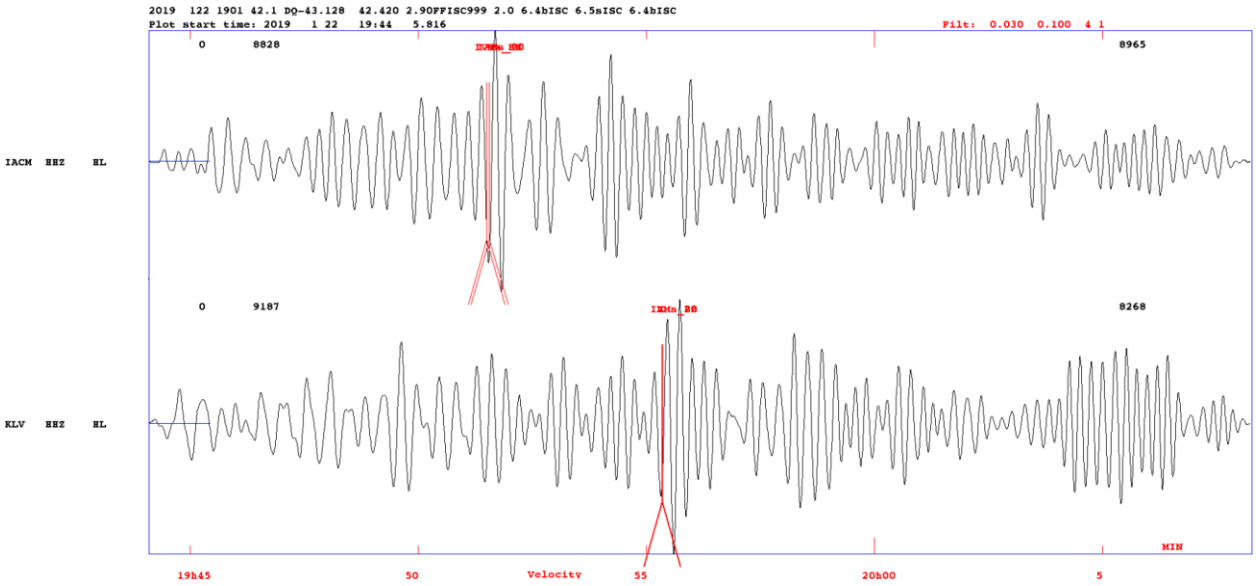

Figure 10: Ground motion of surface waves in terms of velocity (nm/sec), filtered with bandpass filter 0.03-0.1 Hz, stations IACM and KLV reference, event 22/01/2019 19:01:42.

TETR

TETR is located in the northwestern part of Greece at Pindos mountain chain with flysch being the dominating geological formation in the area, IGME geological map, sheet Myrofyllo.

The TETR station has low noise levels at all frequencies. In comparison with the KLV station, it shows an amplitude almost of the order of 2 higher for P waves. Since the noise level appears ok and low this cannot be caused by wrong gain. The surface waves have similar amplitudes, and the residual is close to zero. We conclude the station is ok (Figure 11, Figure 12, Figure 13) and different mb amplitudes are caused by a local site effect. Stations TETR and KLV are located in regions with different geotectonic characteristics. Underneath KLV in Peloponnese, an oceanic slab and mantle wedge is present.

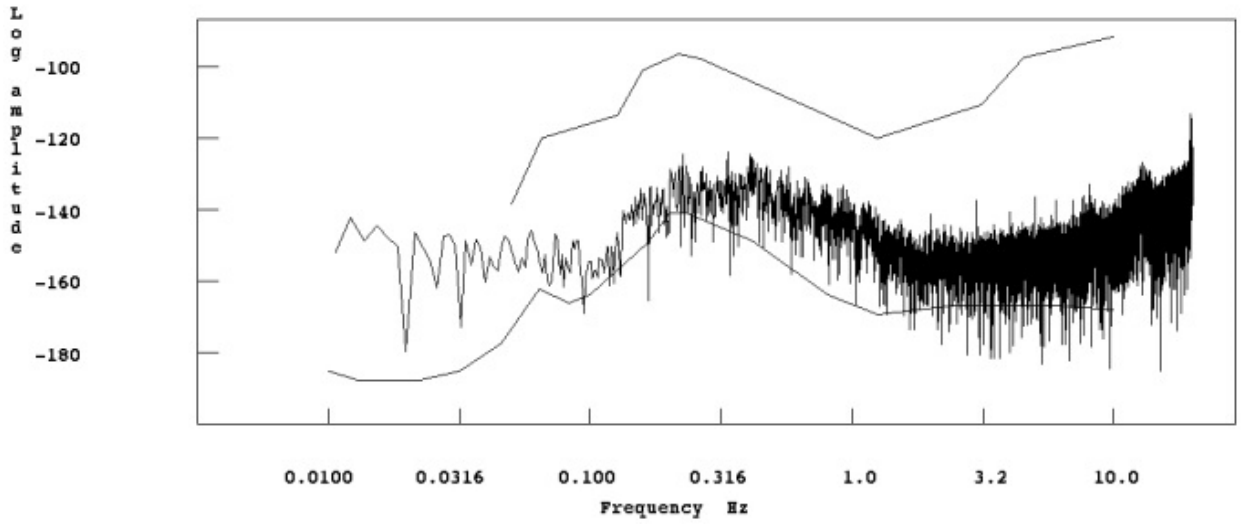

Figure 11: Seismic background noise as acceleration power spectral density in dB relative to (m⁄s^2)^2/Hz. Station TETR, event 28/08/2019 23:46:40. Peterson (1993) curves of the new global high and low noise models are superimposed on the spectrum.

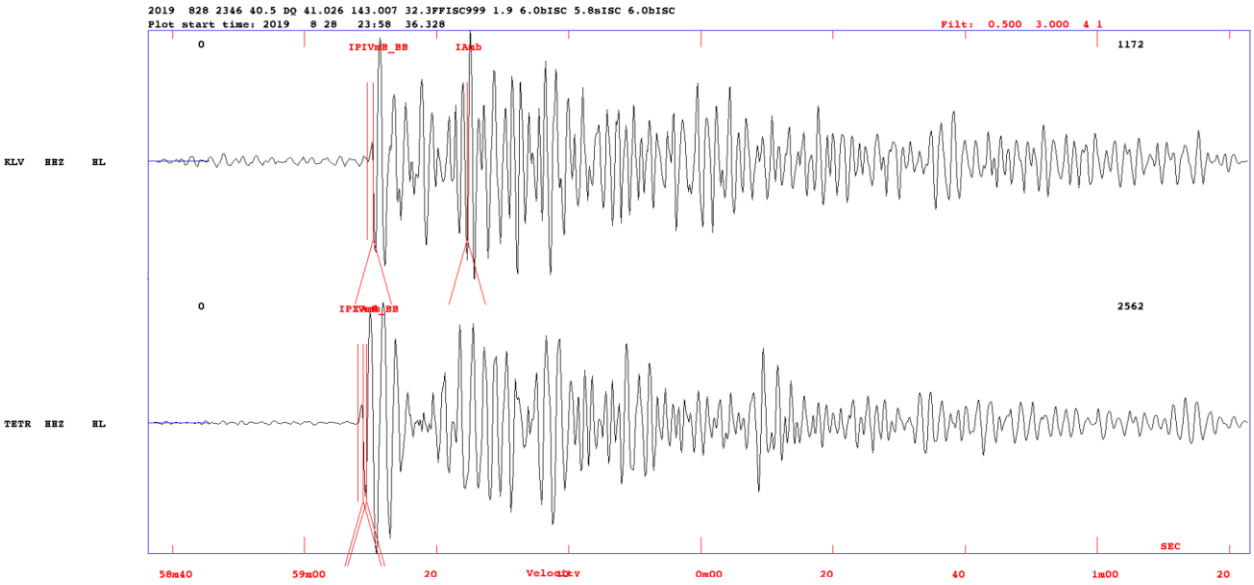

Figure 12: Ground motion around P waves in terms of velocity (nm/sec), filtered with a bandpass filter 0.5-3 Hz, stations TETR and KLV as reference station, event 28/08/2019 23:46:40.

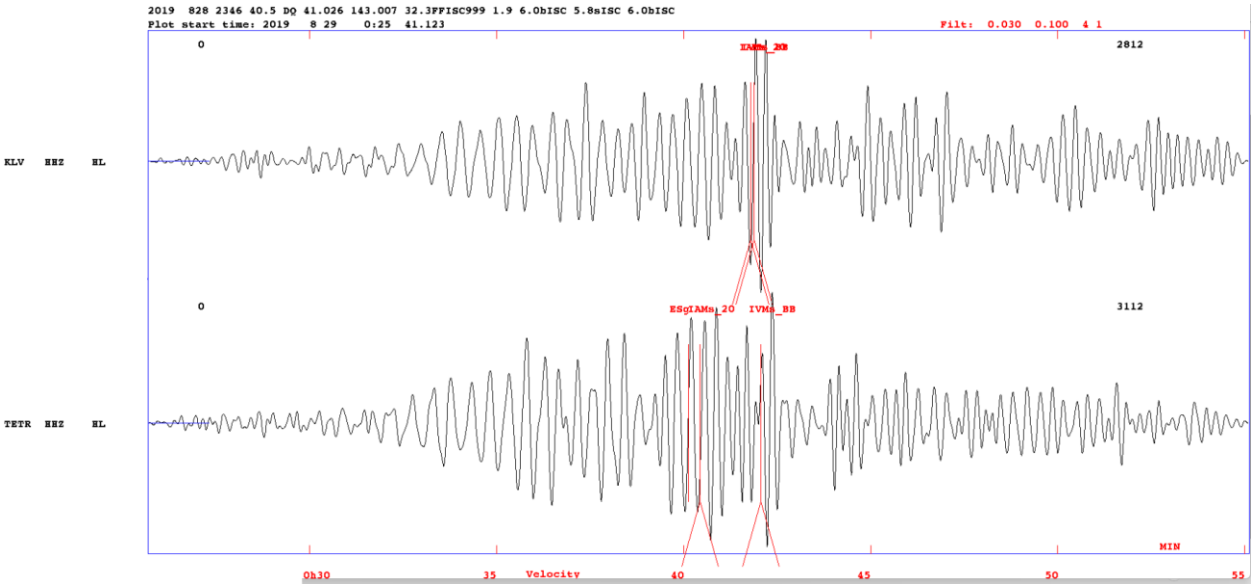

Figure 13: Ground motion on surface waves in terms of velocity (nm/sec), filtered with a bandpass filter 0.03-0.1 Hz, stations TETR and KLV reference, event 28/08/2019 23:46:40.

KARP

KARP belongs to the HL network, it is a remote station located in Karpathos island and seems to operate well. It is installed in a good seismic vault on top of a limestone hill with intense relief. The station shows normal noise level at 0.1-0.3 Hz, low noise level at low frequencies and at higher frequencies the noise levels increase probably because of cultural noise, Figure 14.

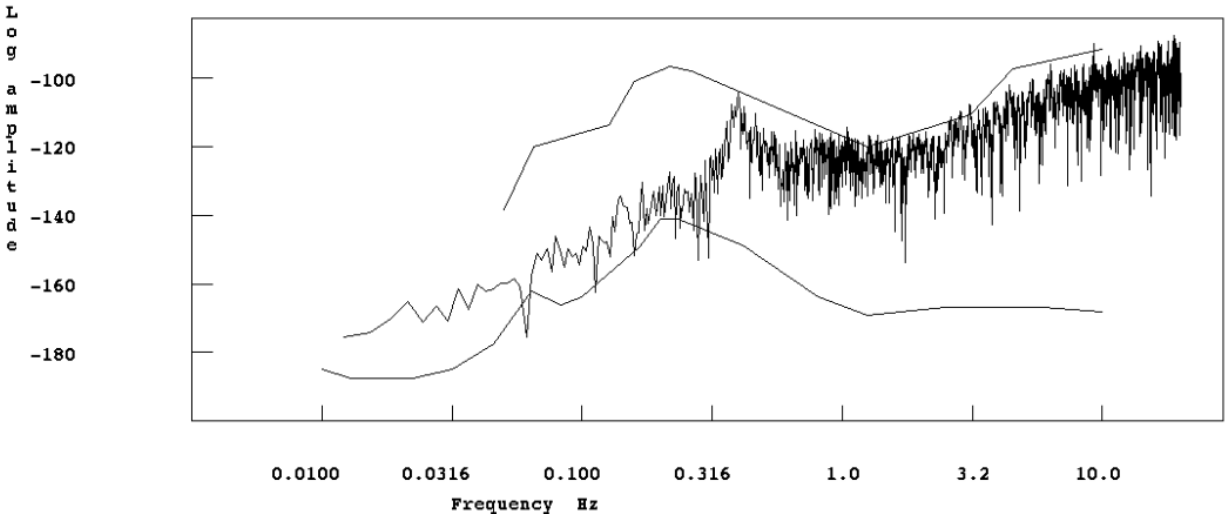

Figure 14: Seismic background noise as acceleration power spectral density in dB relative to (m⁄s^2)^2/Hz . Station KARP, event 28/08/2019 23:46:40. Peterson (1993) curves of the new global high and low noise models are superimposed on the spectrum event.

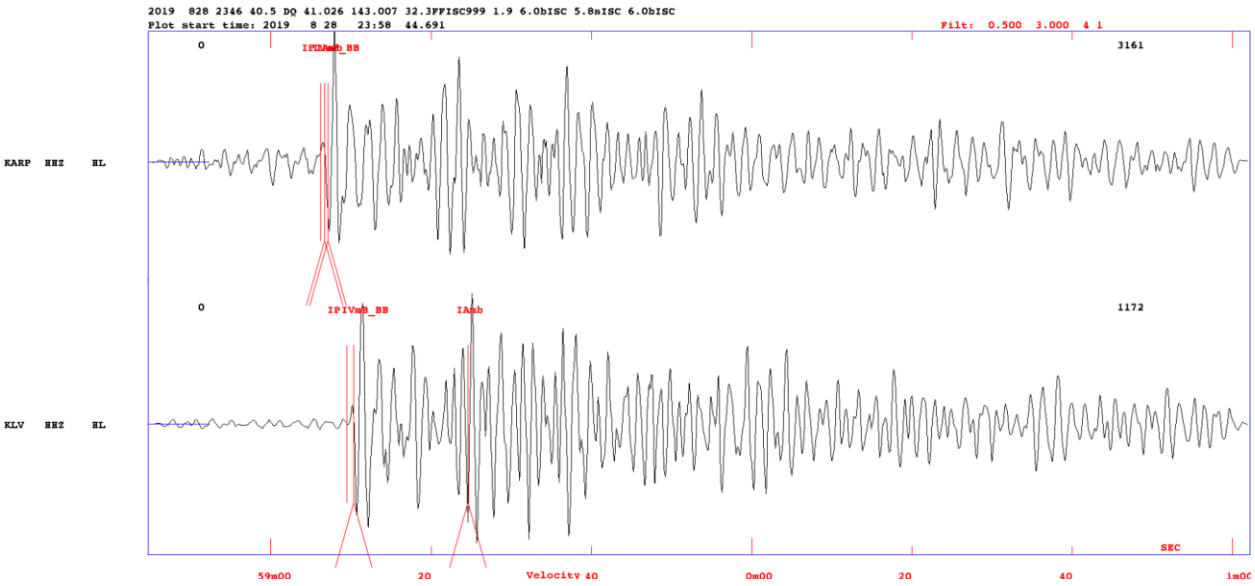

Figure 15: Ground motion around P waves in terms of velocity (nm/sec), filtered with a bandpass filter 0.5-3 Hz, stations KARP and KLV as reference station, event 28/08/2019 23:46:40.

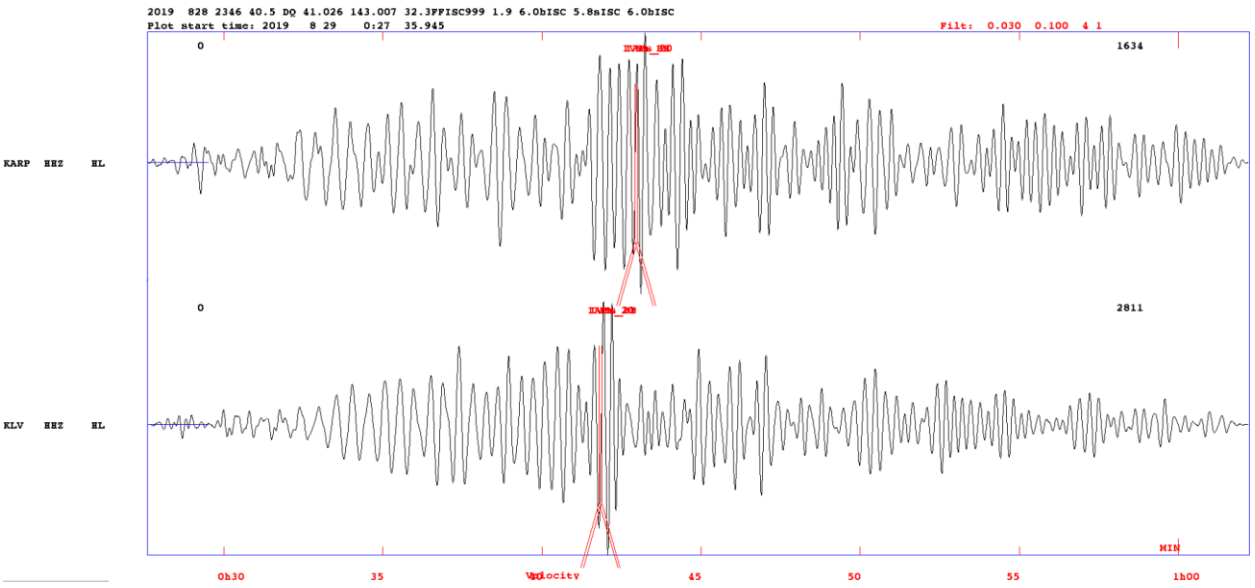

Figure 16: Ground motion on surface waves in terms of velocity (nm/sec), filtered with a bandpass filter 0.03-0.1 Hz, stations KARP and KLV reference, event 28/08/2019 23:46:40.

In comparison with the KLV station, the P wave maximum amplitude of ground motion velocity is significantly higher corresponding to the higher mb, Figure 15. However, the surface waves are similar, so we conclude that the station is ok, Figure 16. Structural differences in the comparisons with KLV station which is also placed on seismic bedrock might be due to topography effects.

ARG

ARG station is located at Archangelos in Rhodes island. The city is extended in a narrow sedimentary basin and the station is placed at the edge of the city, exactly at the foothill of a limestone outcrop. Thus, it can be assumed that it is probably located on seismic bedrock and cultural noise at higher frequencies will be present.

The station is characterized with normal noise levels in the frequency band 0.1-0.3 Hz and intermediate at all the other frequencies, such as 0.01-0.1 Hz and at high frequencies higher than 0.3 Hz, Figure 17.

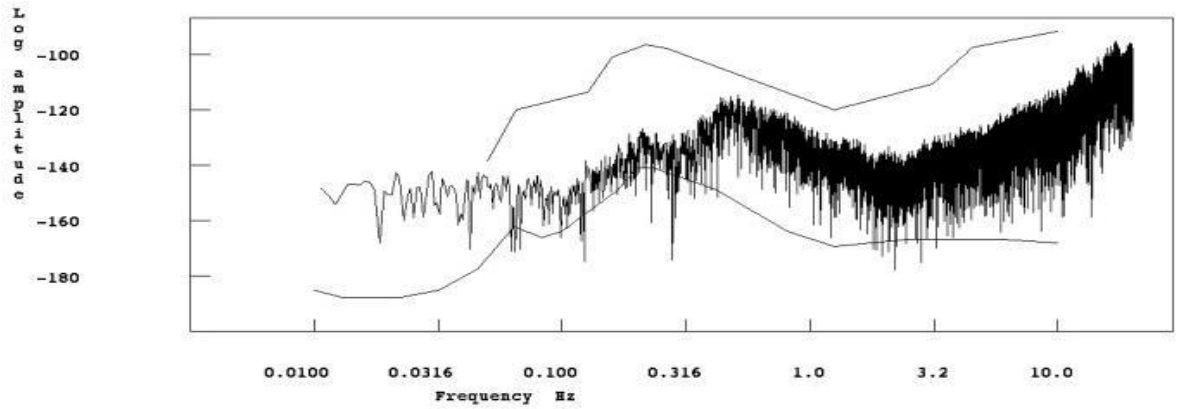

Figure 17: Seismic background noise as acceleration power spectral density in dB relative to (m⁄s^2)^2/Hz . Station ARG, event 01/08/2019 18:28:06. Peterson (1993) curves of the new global high and low noise models are superimposed on the spectrum.

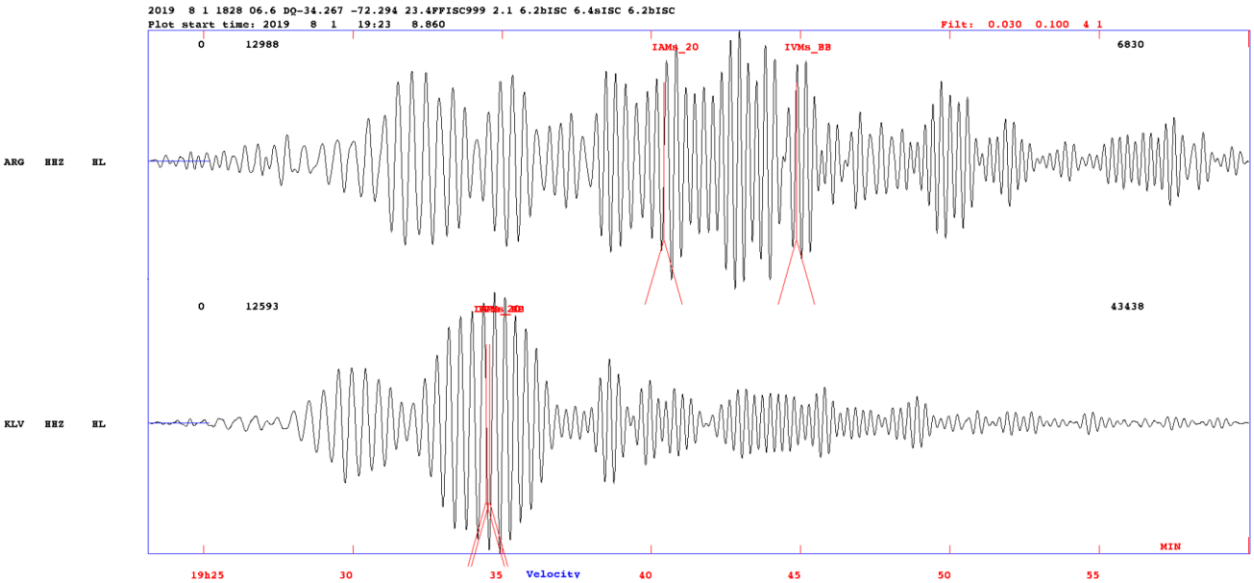

Figure 18: Ground motion on surface waves in terms of velocity (nm/sec), filtered with a bandpass filter 0.03-0.1 Hz, stations ARG and KLV reference, event 01/08/2019 18:28:06.

The amplitude of the surface waves on ARG station are lower in comparison with KLV by an order of six. In this case the P wave onset was very low frequency and magnitude measurements Mb, MB were not

made due to low signal to noise ratio so 0.5-3 Hz comparison could not be made. Comparing the velocity in the 0.01-0.1 Hz range gave the same amplitude as already observed with the surface waves, Figure 18.

In general station ARG magnitude residuals have opposite signs among body waves and surface waves magnitudes. ARG sensor is a Lennartz LE3D-20s so for some long periods of surface waves this can be the reason for lower amplitudes in terms of ground velocity. Consequently, this can be the main cause for magnitude deviations. Any probable structural influence in this case should be checked with more comparisons. The station seems ok.

KNT

KNT is located in northern Greece, at Kentriko village close to the borders, and belongs to HT network. It is placed on gneiss, seismic bedrock and the installation is inside a seismic vault.

The station shows constantly high positive Ms magnitude residuals but the Mb residuals are zero. The noise spectrum in Figure 19, is characterized with intermediate noise levels at higher frequencies but high noise levels at low frequencies 0.01 to 0.1 Hz, overall, the level looks ok. In the filter band 0.5 –3 Hz the ground velocity around P is compared to KLV (Figure 20) and the amplitudes are higher on KNT than KLV which does not correspond to zero mb residuals. On the other hand, the surface wave amplitudes are almost the same (Figure 21). This difference could be due to radiation pattern. We conclude that the station is ok.

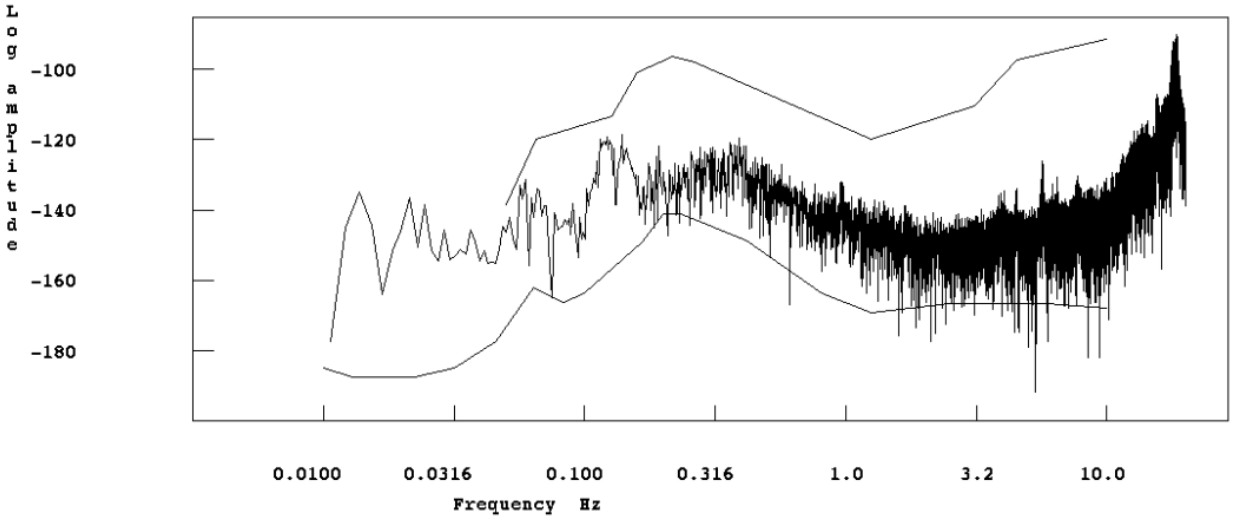

Figure 19: Seismic background noise as acceleration power spectral density in dB relative to (m⁄s^2)^2/Hz . Station KNT, event 22/01/2019 19:01:42. Peterson (1993) curves of the new global high and low noise models are superimposed on the spectrum.

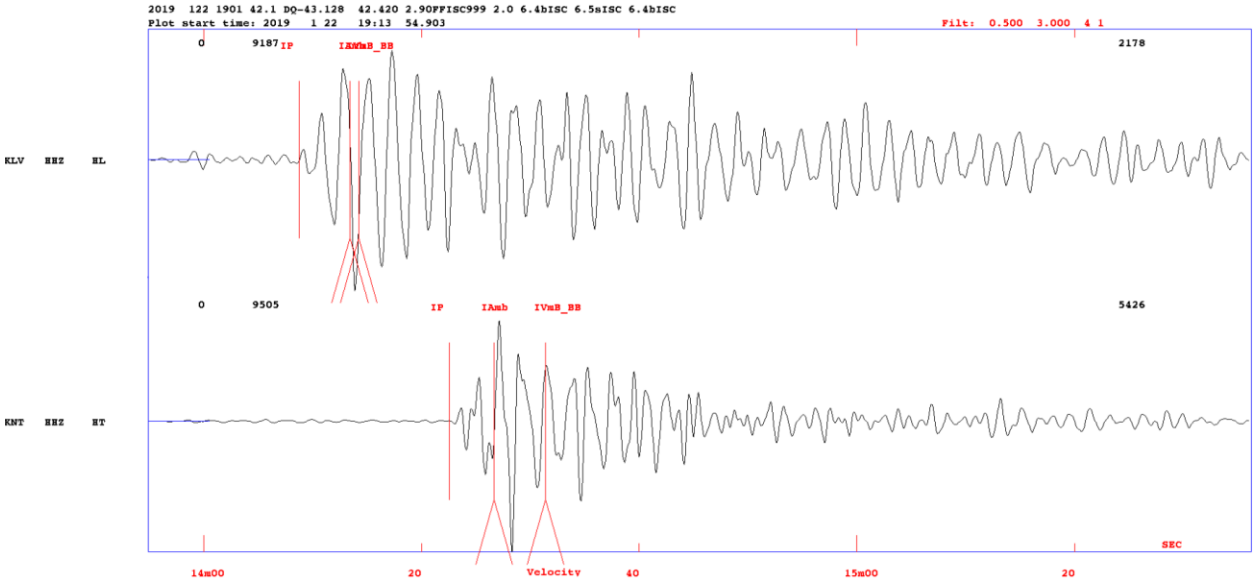

Figure 20: Ground motion around P waves in terms of velocity (nm/sec), filtered with a bandpass filter 0.5-3 Hz, stations KNT and KLV as reference station, event 22/01/2019 19:01:42.

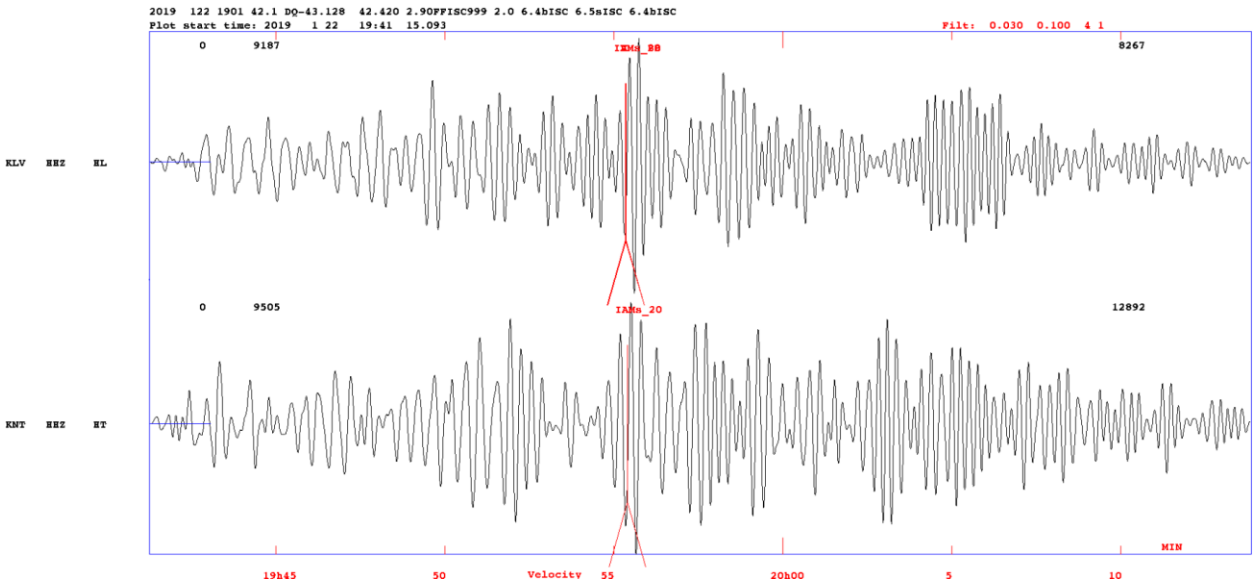

Figure 21: Ground motion on surface waves in terms of velocity (m/sec), filtered with a bandpass filter 0.03-0.1 Hz, stations KNT and KLV reference, event 22/01/2019 19:01:42.

Conclusion

The stations checked do not seem to have instrumental problems but some have high noise levels.

Magnitudes Comparisons

For the analyzed teleseismic events of 2019, comparisons have been conducted between the different magnitudes calculated among the NOA/GI data and additionally comparisons among Mb magnitudes and Ms between ISC and NOA/GI. All magnitude comparisons were made fixed to the ISC Prime Hypocentral solutions. Empirical relations are always calculated with maximum likelihood, a mathematical method to approach best fit.

Compare NOA/GI MS, Ms

In Figure 22, a MS - Ms comparison is presented as derived from the magnitude measurements of the HUSN stations. The Maximum likelihood best fit, is:

MS(NOA) = 0.981 * Ms(NOA) + 0.138 (4)

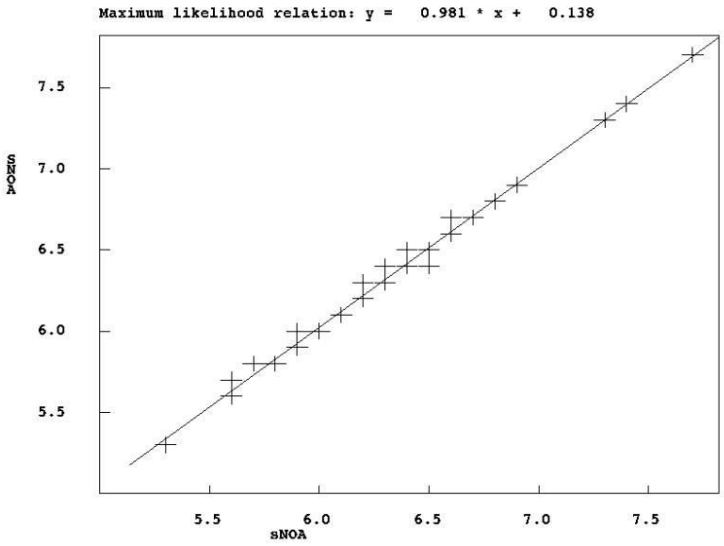

Figure 22: Comparison between surface wave magnitudes broadband MS and Ms of NOA.

With a correlation factor of 0.99 and similar average values of 6.36, 6.38 between Ms and MS respectively, indicates that there is no difference in values between them. These magnitudes are equivalent, and no saturation is expected. Thus, choosing only to measure MS magnitude for the rest of the catalogue could be a good choice.

Compare NOA MB and Mb

Comparison of NOA broadband MB and Mb, is shown in Figure 23.

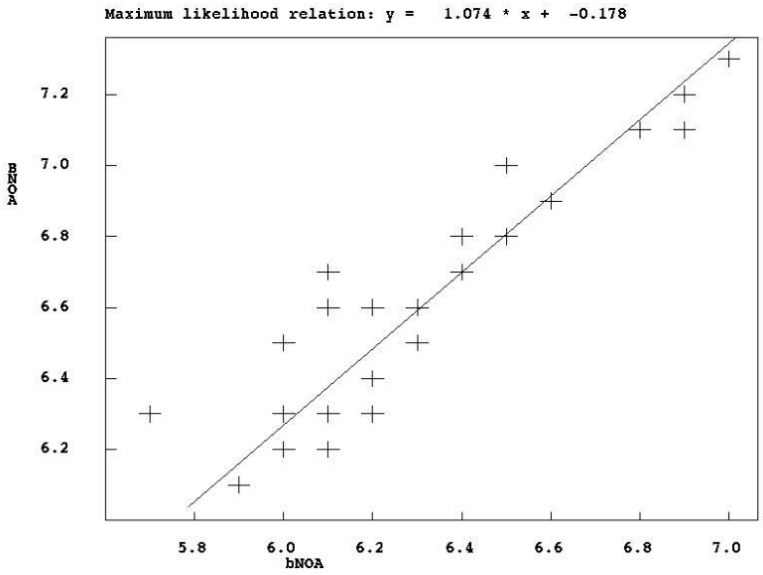

Figure 23: Comparison between body wave magnitudes Mb and broadband MB of NOA.

Average values of magnitudes Mb, MB are 6.26 and 6.55 respectively and the correlation is 0.9. The difference in magnitude indicates that Mb magnitude might saturate, and MB is therefore a better magnitude to use for larger events. For HUSN stations, MB magnitude shows higher values in comparison with all the other magnitude types (Ms, MS, Mb). The maximum likelihood best fit, is:

MB(NOA) = 1.074 * Mb(NOA) + -0.178 (5)

Compare Ms NOA to Ms ISC

Ms should have been read in the period range 18-22s. This has not been done since our software does not do it automatically so some trial and error is needed. Checking the ISC data also shows that many data used by ISC also are outside the range 18-22 s so it is to be expected that there might be differences in Ms, Figure 24, shows the comparison.

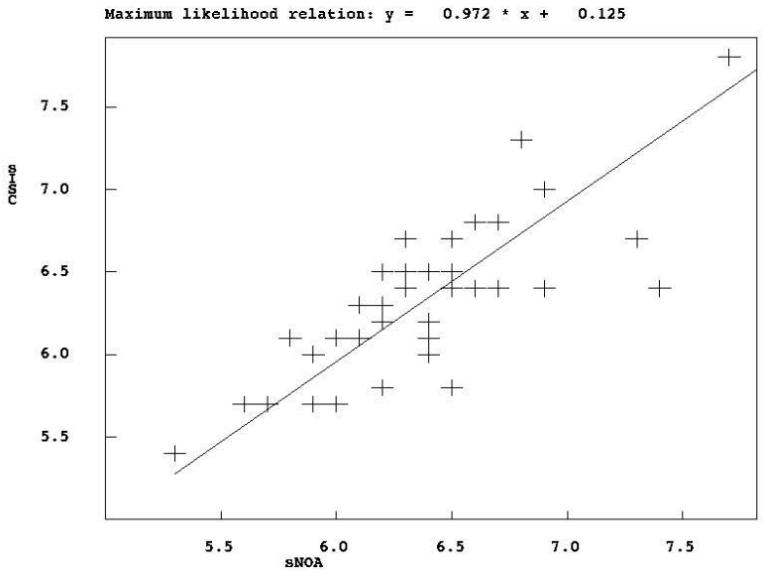

Figure 24: Comparison of Surface waves magnitude Ms, between ISC and NOA.

The average of the 2 datasets for ISC and NOA are 6.32 and 6.37 respectively so on average NOA Ms seems to be correct. However, the data shows quite a bit of scatter, more than one should expect. The Maximum likelihood relation of 2019 is:

Ms(ISC) = 0.972 * Ms (NOA) + 0.125 (6)

An extreme Ms value difference is for the event of **01/08/2019 18:28** with higher values reported by NOA of the order of one magnitude unit (Ms(NOA) 7.4, Ms(ISC) 6.4, Ms(USGS) 6.4). For this event Ms magnitude residuals per station, relative to the NOA Ms magnitude, are plotted with the distance in Km, Figure 25. The most deviating stations are:

STAT	RES	AV RES
ARG	-0.5	-0.3
THERA	-0.6	-0.2
APE	-0.6	-0.2
KNT	+0.4	+0.6

where RES is station residual for the event and AV RES is the average station residual for all events. Stations THERA and APE deviate the most with residuals of -0.6 and then ARG with -0.5, but most of the stations exhibit small variations in magnitude residuals showing good internal consistency. This implies that NOA magnitude calculation is internally consistent and therefore probably correct. In any case this event magnitude is calculated as the average of many stations measurements and will not be affected by a few outlying station measurements. Considering this event, it should be briefly mentioned that station checks were made for THERA and APE too, which revealed lower ground motion amplitudes on surface

waves of THERA station in comparison with KLV station indicating a structural influence. THERA station is located in Santorini volcanic island.

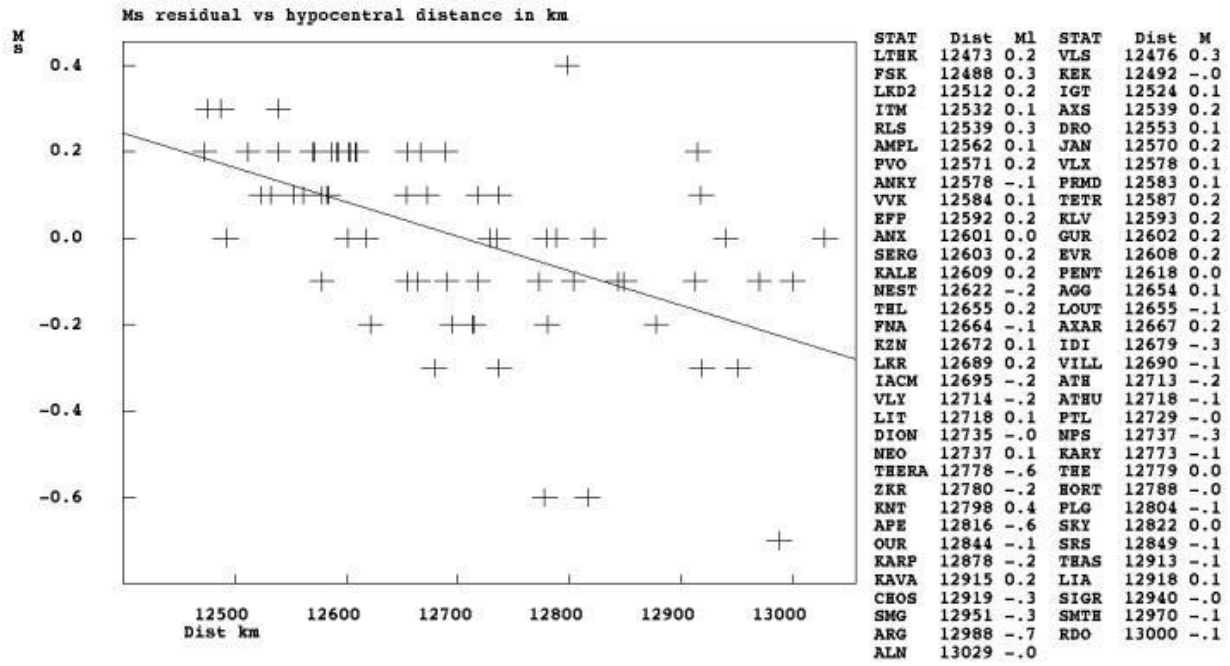

STAT	Dist	Ml	STAT	Dist	M
LTHK	12473	0.2	VLS	12476	0.3
FSK	12488	0.3	KEK	12492	-.0
LKD2	12512	0.2	IGT	12524	0.1
ITM	12532	0.1	AXS	12539	0.2
RLS	12539	0.3	DRO	12553	0.1
AMPL	12562	0.1	JAN	12570	0.2
PVO	12571	0.2	VLX	12578	0.1
ANKY	12578	-.1	PRMD	12583	0.1
VVK	12584	0.1	TETR	12587	0.2
EFP	12592	0.2	KLV	12593	0.2
ANX	12601	0.0	GUR	12602	0.2
SERG	12603	0.2	EVR	12608	0.2
KALE	12609	0.2	PENT	12618	0.0
NEST	12622	-.2	AGG	12654	0.1
THL	12655	0.2	LOUT	12655	-.1
FNA	12664	-.1	AXAR	12667	0.2
KZN	12672	0.1	IDI	12679	-.3
LKR	12689	0.2	VILL	12690	-.1
IACM	12695	-.2	ATH	12713	-.2
VLY	12714	-.2	ATHU	12718	-.1
LIT	12718	0.1	PTL	12729	-.0
DION	12735	-.0	NPS	12737	-.3
NEO	12737	0.1	KARY	12773	-.1
THERA	12778	-.6	THE	12779	0.0
ZKR	12780	-.2	HORT	12788	-.0
KNT	12798	0.4	PLG	12804	-.1
APE	12816	-.6	SKY	12822	0.0
OUR	12844	-.1	SRS	12849	-.1
KARP	12878	-.2	THAS	12913	-.1
KAVA	12915	0.2	LIA	12918	0.1
CHOS	12919	-.3	SIGR	12940	-.0
SMG	12951	-.3	SMTH	12970	-.1
ARG	12988	-.7	RDO	13000	-.1
ALN	13029	-.0			

Figure 25: Magnitude Ms residuals per station for the event of 01/08/2019 18:28.

The magnitude residuals seem to have distance bias which might indicate some regional dependency of the amplitudes. Event is located southwest of Sumatra region and from ATH station that can be assumed relatively close to the center of the network has a distance of 12713 Km.

Other agencies have reported a high Ms for this event like 7.0 (BJI) and Mw is also above 7 for some agencies.

Compare Mb NOA to Mb ISC

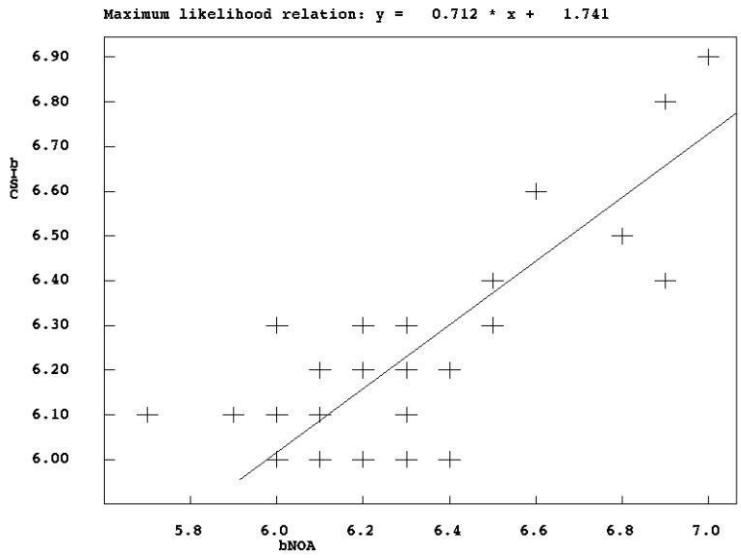

Figure 26: Comparisons of Body waves magnitude Mb, between ISC and NOA.

Considering Mb comparisons between NOA and ISC, (Figure 26), the data correlation seems not so good with a value of 0.79. The average values of the magnitudes are similar (Mb(NOA) av 6.26, Mb(ISC) av 6.20). The best fit line with Maximum likelihood is:

Mb(ISC) = 0.712 * Mb(NOA) + 1.741 (7)

Some events have quite different Mb compared to ISC. The Mb NOA magnitudes measurements of the event **30/05/2019 09:03** shows a difference of 0.4 lower magnitudes Mb reported by NOA compared to the ISC magnitude. This event is generally recorded with a low signal to noise ratio in HUSN stations. On the other hand, other events show higher values by NOA in comparison with the ISC, like the event of **22/01/2019 19:01** with a 0.5 Mb difference (6.4 MbISC, 6.9 MbNOA) and also the events of 12/04/2019 and 28/08/2019. All of these events were examined separately. Magnitude Mb residuals per station versus the distance were plotted for every event. As an example, the event of 22/01/2019 is shown in Figure 27 for the IMMV station is deviating the most with a residual of -0.6. There is no correspondence between IMMV station residual -0.6 for this event and the average station residuals of 0.24 of magnitude Mb, see Appendix II. The majority of residuals are in the range -0.3 to 0.3, which is normal for this type of data.

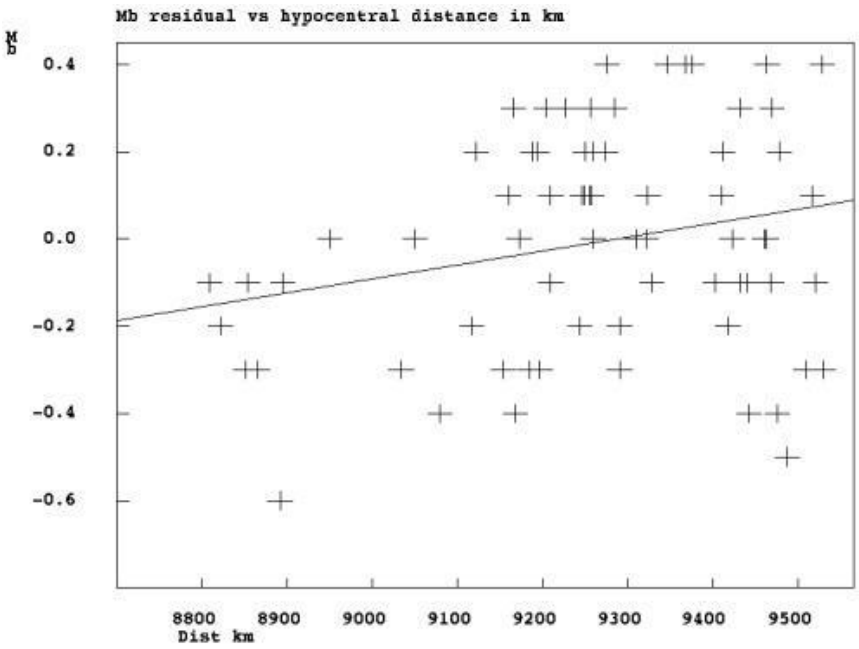

STAT	Dist	Ml	STAT	Dist	M
ZKR	8809	-.1	GVD	8822	-.2
IACM	8852	-.3	IDI	8854	-.1
KSL	8865	-.3	IMMV	8892	-.6
ARG	8895	-.1	ANKY	8950	0.0
APE	9034	-.3	VLI	9050	-.0
SMG	9080	-.4	KRND	9117	-.2
ITM	9122	0.2	VLY	9154	-.3
KARY	9160	0.1	ATHU	9166	0.3
ATH	9168	-.4	PTL	9173	0.0
LOUT	9185	-.3	LTK	9189	0.2
GUR	9194	0.2	VILL	9197	-.3
LTHK	9204	0.3	DRO	9210	-.1
KLV	9210	0.1	RLS	9227	0.3
AXS	9244	-.2	KALE	9247	0.1
SKY	9249	0.1	SERG	9251	0.2
LKR	9256	0.1	PRK	9257	0.3
VVK	9258	0.1	SIGR	9260	0.2
VLS	9260	0.0	ANX	9274	0.2
AXAR	9276	0.4	PVO	9285	0.3
FSK	9291	-.3	PDO	9291	-.2
EVR	9311	0.0	NEO	9322	-.0
LKD2	9324	0.1	XOR	9329	-.1
LIA	9347	0.4	TETR	9369	0.4
THL	9376	0.4	SMTH	9403	-.1
IGT	9411	0.1	JAN	9412	0.2
OUR	9418	-.2	LIT	9423	0.0
KPRO	9432	0.3	THAS	9433	-.1
PLG	9433	-.1	ALN	9440	-.1
KEK	9443	-.4	KZN	9461	0.0
PENT	9463	0.0	HORT	9464	0.4
KOKK	9469	-.1	THE	9470	0.3
RDO	9476	-.4	KAVA	9479	0.2
NEST	9488	-.5	SRS	9510	-.3
GRG	9517	0.1	FNA	9521	-.1
KNT	9529	0.4	NVR	9530	-.3

Figure 27: Magnitude Mb residuals per station for the event of 22/01/2019 that deviates the most from ISC.

Magnitude Mb comparison between NEIC and ISC

Since ISC uses amplitudes for Mb obtained from different agencies which might use different standards, the ISC magnitudes were also compared to the magnitudes from NEIC, which determines all the amplitudes the same way, see Figure 28.

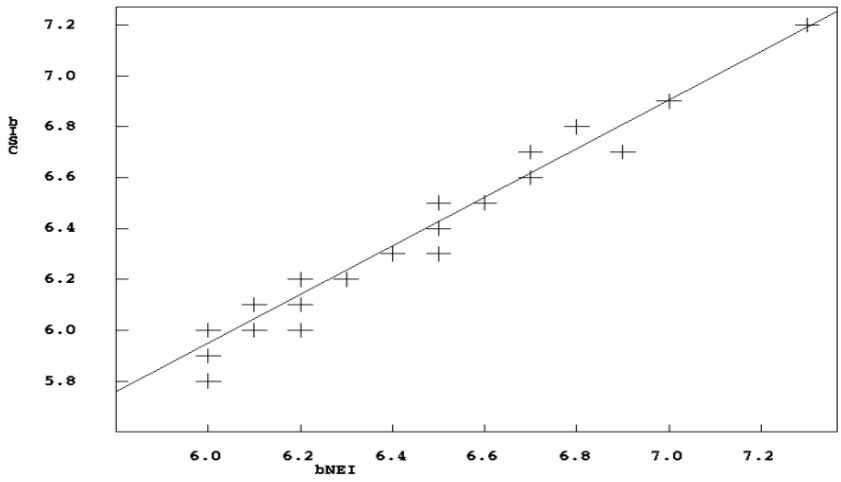

Figure 28: Magnitude Mb comparison between NEIC and ISC.

The Maximum likelihood relation of 2019 among ISC and NEIC, Figure 28, is:

Mb(ISC) = 0.956 * Mb(NEI) + 0.215 (8)

As it can be seen, the magnitudes from ISC and NEIC are very similar, so it is very unlikely that the ISC Mb is not correct and we conclude it is the NOA magnitude deviating. The same can be said for the other strongly deviating events as seen in Table 4.

Table 4: Magnitude Mb comparison between NOA, ISC, and NEIC for the events with most deviation.

Mb Magnitude comparisons					
ID	**Date**	**Time**	**NOA**	**ISC**	**NEIC**
1	22/01/2019	19:01	6.9	6.4	6.5
2	12/04/2019	11:40	6.0	6.3	6.4
3	23/05/2019	8:45	6.3	6.0	6.0
4	30/05/2019	9:03	5.7	6.1	6.2
5	28/08/2019	23:46	6.4	6.0	6.0

Conclusions

Global events of 2019 with Mb magnitude ≥ 6 based on the prime solutions of ISC were analyzed for around one hundred selected broadband stations from the Hellenic Unified Seismic Network. Data analyses included phase characterization, location analyses and magnitude calculations of four different magnitude types, body wave magnitudes Mb, MB and surface wave magnitudes Ms and MS. Statistics were made for comparison purposes and to evaluate the accuracy of analysis. Locations using the data of the HUSN stations, were in good agreement with the ISC prime solutions and any small differences are negligible considering the large teleseismic distances. These results enhanced the accuracy of phase recognition and picking of teleseismic phases such as P, Pdif, PP, PKP, pP, pPKP, pPKP, S, SKS, SS.

Magnitude measurements were conducted following the criteria and restrictions in terms of period, distance and depth as described by the latest IASPEI standards, by Bormann and Dewey, 2014. Comparisons were done between the different magnitude types Mb, MB, Ms, MS calculated by NOA/GI and additionally comparisons among Mb and Ms magnitudes between ISC and NOA/GI. These were conducted fixed to the ISC Prime Hypocenter solutions which revealed similarities and discrete differences. In detail, surface magnitudes Ms and MS of NOA/GI are equivalent, and no saturation is expected. Thus, MS will be calculated for the rest of the catalogue. Magnitude MB exhibits the highest values per event in comparison with the rest of the magnitudes Mb, Ms, MS. NOA/GI broadband magnitudes MB and MS are stable with higher internal consistency in comparison with magnitudes Mb, Ms.

The comparison of magnitude Mb among NOA/GI and ISC concerning some events revealed significant discrepancies. Stations with large magnitude residuals for these events were checked further in terms of noise and amplitudes were compared to the good reference station KLV. Stations IACM, KNT, APE, ARG had large magnitude residuals, however they seem to have no gain problems. The THERA station showed a strong site effect on surface waves.

This work has set up the basis for processing the remaining 9 years of the teleseismic data. Completing this task with events with sufficient global coverage will give a better understanding of the network characteristics, and also be the basis for more research. The analyses showed that HUSN broadband stations have good recordings of global events at all teleseismic distances and can contribute to the number of stations reporting phases and amplitudes from large earthquake events. Additionally, the data will contribute to the global database with a large amount of different magnitude measurements especially for MB that it is not often reported by other agencies.

Acknowledgments:

This work was enhanced significantly with the valuable input and guidance provided by Dr. C. Evangelidis (project member) through his special comments and instructions. Special thanks to Dr. Olga-Joan Ktenidou for her participation as an integral member of the project team and her significant contribution during the drafting proposal. Following the implementation of this catalogue, their collaboration and expertise are expected to greatly benefit this research and expand the upcoming research activities.

Appendix I: *Teleseismic events for the year 2019 with magnitude Mb ≥6 analyzed with Greek stations. Magnitudes and hypocenters are from ISC. Lat, Lon, Depth, rms, Magn columns refers to the ISC solutions. Phase Types refers to the phase recognition for Greek stations after locating the events. Magnitude Types and comments describe what type of magnitudes and why were calculated per event.*

No	Date	Time	Lat	Lon	Depth	rms	Magn	Phase Types	Magn Types	comments
1	5/1/2019	19:25:38	-8.180	-71.644	583.5	2.1	6.3bISC	Pdif,pP,SKSac, SS	No magnitudes	Event too far & Deep >60 Km
2	6/1/2019	17:27:19	2.304	126.715	48.4	1.9	6.2bISC	P,Pdif,SKSac	Ms,MS,Mb,MB	
3	20/1/2019	1:32:51	-30.077	-71.318	65.5	1.8	6.5bISC	Pdif,PP,SS	No magnitudes	Event too far & Deep >60 Km
4	22/1/2019	5:10:05	-10.288	119.130	34.7	2.2	6.0bISC	P,Pdif,PP,SKSac	Ms,MS	Event too far, no Mb,MB
5	22/1/2019	19:01:42	-43.128	42.420	2.90	2.0	6.4bISC	P,PP,S,SS	Ms,MS,Mb,MB	
6	26/1/2019	8:12:50	-5.562	133.799	28.6	1.4	6.1bISC	**not analysed**		Low frequency event, Low signal/noise ratio
7	1/2/2019	16:14:12	14.771	-92.279	78.1	2.3	6.1bISC	P,Pdif,PP,SKSac	No magnitudes	Event too far & Deep >60 Km
8	2/2/2019	9:27:35	-2.762	100.194	18.0	1.7	6.0bISC	P,S	Ms,MS,Mb,MB	
9	8/2/2019	11:55:08	9.790	126.387	28.0	1.6	6.2bISC	P	Ms,MS	Event too far, no Mb,MB
10	17/2/2019	14:35:55	-3.435	152.183	374.6	1.7	6.3bISC	PKPdf,pPKPdf,PP,SS	No magnitudes	Event too far & Deep >60 Km
11	22/2/2019	10:17:22	-2.276	-77.007	149.9	1.7	6.8bISC	P,Pdif,pP,PP,SS	few Mb,MB	Event too far & Deep >60 Km
12	1/3/2019	8:50:42	-14.683	-70.058	265.2	2.2	6.7bISC	P,pP,PP,SKSac	No magnitudes	Event too far & Deep >60 Km
13	2/3/2019	3:22:53	41.985	146.939	19.0	1.7	6.0bISC	P,PP,SKSac	Ms,MS,Mb,MB	
14	6/3/2019	15:46:13	-32.060	-177.839	26.3	1.8	6.0bISC	PKP,PP	few Ms,MS	Event too far >17500 Km, no Mb,MB
15	24/3/2019	4:37:35	1.680	126.275	45.5	1.6	6.1bISC	P,Pdif	Ms,MS	Event too far, no Mb,MB
16	28/3/2019	22:06:49	50.421	160.021	14.5	1.5	6.2bISC	P,SKSac	Ms,MS,Mb,MB	
17	2/4/2019	21:35:31	52.059	177.998	11.6	2.1	6.2bISC	P,PP,SKSac	Ms,MS,Mb,MB	
18	5/4/2019	16:14:16	-55.954	-27.888	62.3	1.7	6.2bISC	PP,SS	No magnitudes	Event too far & Deep >60 Km
19	9/4/2019	17:53:59	-58.587	-25.442	47.9	2.0	6.5bISC	Pdif,PP	Ms,MS	Event too far, no Mb,MB
20	12/4/2019	11:40:49	-1.808	122.572	19.6	1.8	6.3bISC	P,Pdif,SKSac	Ms,MS,Mb,MB	
21	18/4/2019	5:01:05	24.053	121.620	13.9	1.8	6.2bISC	P,PP,S	Ms,MS,Mb,MB	
22	22/4/2019	9:11:11	14.906	120.476	21.9	1.4	6.0bISC	P,PP,SKSac	Ms,MS,Mb,MB	
23	23/4/2019	5:37:53	11.768	125.150	67.7	1.7	6.3bISC	P,pP, PP, SKSac	Mb,MB	Deep event >60 Km, no Ms, MS
24	3/5/2019	7:25:30	-6.873	160.102	23.7	1.3	6.2bISC	PKPdf, PP,SKPbc	Ms,MS	Event too far, no Mb,MB
25	6/5/2019	21:19:37	-6.997	146.445	140.4	1.9	6.7bISC	Pdif , PP,SS	No magnitudes	Event too far & Deep >60 Km
26	14/5/2019	12:58:26	-4.199	152.620	15.7	2.6	6.5bISC	Pdif,PKPdf,pPKPdf,PP,SS	Ms,MS	Event too far, no Mb,MB
27	22/5/2019	0:39:34	13.807	93.014	30.6	1.6	6.0bISC	P,pP,S	Ms,MS,Mb,MB	
28	23/5/2019	8:45:18	51.402	-178.288	40.3	1.6	6.0bISC	P, pP, PP, SKSac	Ms,MS,Mb,MB	
29	26/5/2019	7:41:14	-5.893	-75.246	125.5	1.7	7.2bISC	Pdif,pP,pPdif,PP,SKS	No magnitudes	Event too far & Deep >60 Km
30	30/5/2019	9:03:29	13.212	-89.270	61.2	2.2	6.1bISC	Pdif,pP,PP,SKSac	Mb,MB	Deep event >60 Km, no Ms, MS
31	31/5/2019	10:12:31	6.260	126.537	93.2	1.5	6.1bISC	Pdif,pP,PP,SKSac	Mb,MB	Deep event >60 Km, no Ms, MS
32	4/6/2019	4:39:17	29.067	139.279	437.2	1.6	6.2bISC	P,pP,PP,SKSac	Mb,MB	Deep event >60 Km, no Ms, MS

33	14/6/2019	20:10:54	-5.868	130.762	131.4	1.5	6.0bISC	Pdif	No magnitudes	Event too far & Deep >60 Km
34	15/6/2019	22:55:02	-30.808	-178.025	38.5	2.1	6.7bISC	PKPdf,pPKPdf,PP,few SS	No magnitudes	Event too far >17500 Km
35	18/6/2019	13:22:21	38.623	139.471	17.8	2.0	6.4bISC	P,PP,SKSac	Ms,MS,Mb,MB	
36	19/6/2019	7:01:44	-30.696	-177.848	23.2	2.3	6.1bISC	PKPdf,PP,SS	No magnitudes	Event too far >17500 Km
37	24/6/2019	2:53:39	-6.389	129.247	221.2	2.0	6.7bISC	Pdif,PP few,SKSac	No magnitudes	Event too far & Deep >60 Km
38	25/6/2019	9:05:41	56.146	164.188	18.7	1.8	6.0bISC	P,S	Ms,MS,Mb,MB	
39	26/6/2019	2:18:08	56.136	164.122	12.9	1.4	6.2bISC	P,S	Ms,MS,Mb,MB	
40	28/6/2019	15:51:32	19.865	144.402	437.9	1.7	6.0bISC	Pdif,PP few,SKSac	Mb,MB	Deep event >60 Km, no Ms, MS
41	7/7/2019	15:08:41	0.460	126.119	43.7	2.0	6.6bISC	Pdif,pP few, SKSac	Mb,MB	Deep event >60 Km, no Ms, MS
42	14/7/2019	5:39:25	-18.268	120.438	19.6	2.0	6.2bISC	Pdif, PP,SS	Ms,MS	Event too far, no Mb,MB
43	14/7/2019	9:10:51	-0.612	128.095	13.7	2.3	6.3bISC	Pdif, PP,SS	Ms,MS	Event too far, no Mb,MB
44	31/7/2019	15:02:33	-16.215	168.078	187.8	1.6	6.1bISC	PKPdf,pPKPdf,PP	No magnitudes	Event too far & Deep >60 Km. High residuals
45	1/8/2019	18:28:06	-34.267	-72.294	23.4	2.1	6.2bISC	Pdif,PP,SS	Ms,MS	Event too far, no Mb,MB
46	2/8/2019	12:03:26	-7.269	104.855	52.3	1.8	6.5bISC	P,pP,PP,SKSac,SS	Ms,MS,Mb,MB	
47	4/8/2019	10:23:03	37.684	141.595	40.3	1.9	6.2bISC	P,pP,PP,SKSac	Ms,MS,Mb,MB	
48	6/8/2019	22:14:14	-17.979	168.628	157.7	1.3	6.1bISC	PKPdf,PKPbc, few PP	No magnitudes	Event too far & Deep >60 Km
49	8/8/2019	0:45:25	36.491	70.129	226.1	1.7	6.1bISC	P,pP,S	Mb,MB	Deep event >60 Km, no Ms, MS
50	27/8/2019	23:55:21	-60.185	-26.737	30.6	2.1	6.5bISC	Pdif, PP, S, SS	Ms,MS	Event too far, no Mb,MB
51	28/8/2019	23:46:40	41.026	143.007	32.3	1.9	6.0bISC	P,pP, PP,S, SKSac	Ms,MS,Mb,MB	
52	29/8/2019	15:07:58	43.394	-128.069	9.70	2.0	6.1bISC	P few, PP few	Ms,MS,few Mb,MB	Event too far
53	1/9/2019	15:54:21	-20.485	-178.470	611.1	1.5	6.1bISC	PKPdf	No magnitudes	Event too far & Deep >60 Km
54	21/9/2019	19:53:12	-6.533	130.478	73.5	1.8	6.1bISC	**not analysed**		Low frequency event, Low signal/noise ratio
55	25/9/2019	23:46:44	-3.540	128.389	23.4	2.1	6.0bISC	Pdif, PP, SKSac,SS	Ms,MS	Event too far, no Mb,MB
56	27/9/2019	12:05:02	-30.239	-177.904	36.0	1.6	6.1bISC	PKPdf,pPKPdf,PP	No magnitudes	Event too far > 17300 Km
57	29/9/2019	2:02:52	5.662	126.471	84.0	1.9	6.3bISC	P, Pdif	Mb,MB	Deep event >60 Km, no Ms, MS
58	29/9/2019	15:57:54	-35.462	-72.929	15.1	1.9	6.3bISC	Pdif,PKPdf,PP,SS	Ms,MS	Event too far, no Mb,MB
59	16/10/2019	11:37:06	6.778	125.074	17.8	1.9	6.0bISC	P,SKS	Ms,MS,Mb,MB	
60	21/10/2019	2:52:29	-19.136	169.555	236.0	1.6	6.3bISC	PKPdf,PKPbc,PP	No magnitudes	Event too far > 1500 Km
61	29/10/2019	1:04:44	6.730	125.081	22.1	2.1	6.2bISC	P, pP, PP few SKS	Ms,MS,Mb,MB	
62	31/10/2019	1:11:19	6.918	125.264	15.5	1.9	6.2bISC	P,PP,SKS	Mb,MB	Deep event >60 Km, no Ms, MS
63	2/11/2019	18:08:42	-55.735	-26.389	12.5	2.0	6.2bISC	Pdif,PP,SS	Ms,MS	Event too far, no Mb,MB
64	4/11/2019	21:53:24	-31.781	-71.342	51.9	1.6	6.2bISC	**not analysed**		Low frequency event, Low signal/noise ratio
65	4/11/2019	22:43:32	-18.641	-175.287	12.5	2.0	6.0bISC	**not analysed**		Low frequency event, Low signal/noise ratio
66	6/11/2019	0:39:11	-13.656	167.908	22.1	1.4	6.0bISC	**not analysed**		Low frequency event, Low signal/noise ratio
67	8/11/2019	10:44:45	-21.964	-179.428	600.8	1.5	6.0bISC	PKPdf,pPKPdf,PP,SS	No magnitudes	Event too far > 16800 Km

68	14/11/2019	16:17:42	1.564	126.328	48.7	2.0	6.9bISC	P,Pdif,PP,SKSac	Ms,MS,Mb,MB	
69	14/11/2019	21:12:55	1.612	126.399	30.8	1.8	6.0bISC	P,Pdif	Ms,MS,few Mb,MB	
70	20/11/2019	4:27:04	13.777	-93.201	19.7	2.2	6.2bISC	Pdif,SKS	Ms,MS	
71	24/11/2019	0:54:02	51.446	-175.634	32.5	1.7	6.0bISC	P,PP,SKS	Ms,MS,Mb,MB	
72	26/11/2019	2:54:12	41.448	19.632	18.0	2.1	6.2bISC	**not analysed**		Local event
73	27/11/2019	7:23:41	35.775	23.267	70.4	2.0	6.1bISC	**not analysed**		Local event
74	15/12/2019	6:11:51	6.594	125.245	24.2	2.7	6.2bISC	P,SKS	MS,Ms, few MB,Mb	Event too far
75	20/12/2019	11:39:51	36.479	70.561	211.0	1.5	6.1bISC	P, few pP,S	Mb,MB	Deep event >60 Km, no Ms, MS
76	24/12/2019	16:43:32	-26.929	-63.404	568.6	1.6	6.2bISC	**not analysed**		Low frequency event, Low signal/noise ratio

Appendix II: *Average magnitude residuals per stations of HUSN for all type of magnitudes calculated, MB, Mb, MS and Ms. Residuals were defined as the difference between the average event magnitude and the station magnitude. N is the number of station measurements; AV is the average magnitude residual and SD standard deviation.*

	Magnitude Mb			**Magnitude MB**			**Magnitude Ms**			**Magnitude MS**		
STAT	**N**	**AV**	**SD**	**N**	**AV**	**SD**	**N**	**AV**	**SD**	**N**	**AV**	**SD**
ATH	26	0.00	0.21	-	-	-	-	-	-	-	-	-
ZKR	25	0.10	0.19	24	0.05	0.14	35	0.00	0.17	36	0.01	0.17
GVD	23	0.05	0.20	22	0.10	0.14	37	0.00	0.14	33	0.00	0.14
IACM	13	0.47	0.31	13	0.23	0.22	26	-0.30	0.21	34	-0.20	0.22
IDI	25	-0.10	0.27	26	-0.10	0.13	37	-0.10	0.17	36	-0.10	0.17
KSL	16	-0.10	0.25	16	0.00	0.15	33	0.05	0.11	30	0.04	0.11
IMMV	18	0.24	0.28	17	0.19	0.16	20	-0.10	0.14	18	-0.10	0.17
ARG	22	0.21	0.19	23	0.14	0.18	36	-0.30	0.15	20	-0.30	0.16
ANKY	23	0.03	0.17	24	0.05	0.10	33	-0.10	0.11	30	0.00	0.11
APE	15	-0.20	0.31	17	-0.20	0.17	34	-0.10	0.13	31	-0.10	0.11
VLI	24	0.03	0.21	25	0.07	0.12	33	0.11	0.08	28	0.13	0.10
SMG	14	0.00	0.29	15	0.00	0.20	23	-0.10	0.11	23	-0.10	0.11
KRND	11	-0.10	0.22	11	0.00	0.14	16	-0.10	0.11	15	0.00	0.11
ITM	27	0.17	0.22	28	0.07	0.15	39	-0.10	0.09	37	0.00	0.07
VLY	25	-0.10	0.21	26	0.00	0.15	38	-0.10	0.10	38	-0.10	0.09
KARY	22	-0.10	0.25	22	0.00	0.12	15	0.02	0.13	26	0.04	0.10
ATHU	27	-0.10	0.20	27	-0.10	0.11	27	-0.10	0.09	30	-0.10	0.09
ATH	-	-	-	25	0.02	0.14	38	-0.10	0.10	38	-0.10	0.10
PTL	30	0.00	0.25	30	0.00	0.13	35	0.00	0.11	32	0.00	0.09
LOUT	16	-0.20	0.11	17	-0.20	0.11	15	-0.10	0.11	17	0.00	0.07
LTK	23	-0.20	0.16	24	-0.20	0.12	33	-0.10	0.08	35	-0.10	0.07
GUR	24	0.04	0.23	23	0.00	0.16	34	-0.10	0.10	26	-0.10	0.10
VILL	28	-0.20	0.19	27	-0.20	0.10	17	0.12	0.65	15	-0.10	0.12
LTHK	21	0.11	0.22	20	0.06	0.12	33	0.03	0.11	25	0.04	0.12
DRO	22	0.16	0.23	22	0.15	0.17	33	-0.10	0.12	33	0.00	0.11
KLV	25	0.00	0.28	25	0.00	0.18	39	-0.10	0.11	38	-0.10	0.10

RLS	25	0.25	0.27	27	0.18	0.19	32	0.09	0.11	33	0.10	0.10
AXS	24	0.00	0.19	25	0.02	0.12	33	0.01	0.11	29	0.00	0.11
KALE	22	-0.10	0.22	23	-0.10	0.12	23	0.05	0.47	25	0.00	0.09
SKY	26	0.24	0.26	25	0.15	0.16	37	0.02	0.10	38	0.03	0.10
SERG	27	-0.10	0.20	27	-0.10	0.13	38	0.00	0.09	38	0.00	0.08
LKR	27	0.00	0.23	27	-0.10	0.14	35	0.01	0.08	24	0.00	0.08
PRK	21	0.13	0.18	21	0.08	0.09	30	-0.10	0.09	30	-0.10	0.09
VVK	24	0.16	0.23	25	0.07	0.14	35	-0.10	0.12	32	-0.10	0.10
SIGR	25	-0.10	0.25	25	0.00	0.11	38	-0.10	0.10	38	-0.10	0.09
VLS	22	0.12	0.22	24	0.06	0.15	39	0.02	0.12	37	0.03	0.12
ANX	27	-0.10	0.22	26	-0.10	0.13	37	-0.10	0.11	39	-0.10	0.10
AXAR	25	0.03	0.18	26	0.01	0.13	32	0.02	0.09	24	0.03	0.08
PVO	20	0.07	0.19	23	0.09	0.09	34	0.08	0.08	34	0.09	0.07
PDO	10	0.15	0.24	10	0.13	0.11	10	0.06	0.13	9	0.06	0.17
FSK	20	0.11	0.18	20	0.08	0.12	29	0.03	0.13	29	0.03	0.13
EVR	27	0.02	0.23	26	0.00	0.17	38	0.03	0.09	34	0.03	0.08
NEO	26	0.00	0.19	28	0.00	0.11	37	0.00	0.09	38	0.00	0.09
LKD2	25	0.16	0.19	25	0.16	0.12	35	0.04	0.11	35	0.06	0.10
XOR	7	-0.10	0.32	7	-0.10	0.15	12	0.12	0.69	12	-0.10	0.05
LIA	16	0.06	0.37	16	0.07	0.20	31	0.09	0.21	32	0.08	0.20
TETR	26	0.31	0.23	28	0.20	0.14	33	0.06	0.10	37	0.04	0.12
THL	23	-0.30	0.27	23	-0.20	0.14	38	0.03	0.11	39	0.03	0.10
SMTH	25	-0.20	0.21	26	-0.10	0.14	39	0.00	0.10	37	0.00	0.10
IGT	23	0.00	0.21	23	0.03	0.12	38	0.05	0.11	38	0.06	0.10
JAN	24	0.13	0.20	25	0.09	0.13	39	0.10	0.12	35	0.11	0.12
OUR	26	-0.10	0.20	30	0.00	0.08	38	0.00	0.10	39	0.00	0.08
LIT	17	-0.10	0.17	17	0.00	0.12	28	0.01	0.09	29	0.00	0.09
KPRO	11	0.06	0.25	10	0.00	0.18	14	0.07	0.11	13	0.08	0.10
THAS	21	-0.10	0.19	22	-0.10	0.14	32	0.00	0.11	33	0.00	0.11
PLG	19	-0.10	0.19	19	0.00	0.12	23	0.14	0.12	25	0.18	0.21
ALN	29	-0.10	0.17	28	-0.10	0.12	35	0.00	0.10	36	0.00	0.11
KEK	18	0.00	0.26	21	0.03	0.20	37	0.10	0.11	38	0.10	0.11
KZN	22	-0.10	0.18	20	-0.10	0.10	38	0.11	0.10	38	0.10	0.11
PENT	18	-0.10	0.30	20	0.00	0.21	20	0.14	0.20	20	0.17	0.16
HORT	29	-0.30	0.21	30	-0.20	0.09	39	0.06	0.11	39	0.04	0.11
KOKK	15	-0.10	0.15	15	-0.10	0.10	17	0.00	0.08	17	-0.10	0.07
THE	26	-0.20	0.22	26	-0.10	0.16	22	0.12	0.16	16	0.13	0.13
RDO	27	-0.10	0.29	28	-0.10	0.18	36	0.00	0.13	38	0.00	0.14
KAVA	29	0.15	0.22	30	0.15	0.10	31	0.20	0.12	35	0.21	0.10
NEST	19	-0.10	0.27	19	-0.10	0.14	32	0.04	0.14	34	0.05	0.11
SRS	28	-0.10	0.18	29	-0.10	0.09	37	0.03	0.12	38	0.04	0.11
GRG	12	0.11	0.21	12	0.07	0.14	17	0.08	0.12	16	0.06	0.12
FNA	15	-0.20	0.15	14	-0.20	0.09	19	0.07	0.12	16	0.08	0.11
KNT	30	0.00	0.23	30	0.11	0.16	30	0.63	0.14	3	0.74	0.08

NVR	4	-0.30	0.29	4	-0.20	0.10	6	0.06	0.07	6	0.05	0.07
DION	21	-0.10	0.24	24	-0.10	0.15	29	-0.10	0.10	22	-0.10	0.11
PAIG	13	0.06	0.21	14	0.01	0.11	18	0.00	0.09	18	0.00	0.07
VLX	23	-0.20	0.21	23	-0.20	0.10	31	-0.10	0.11	27	-0.10	0.09
EFP	25	0.04	0.26	26	0.02	0.13	21	0.00	0.13	27	0.03	0.10
KARP	23	0.31	0.28	23	0.26	0.21	36	0.00	0.18	34	0.01	0.18
AGG	21	-0.10	0.22	21	-0.10	0.12	28	0.03	0.07	29	0.04	0.06
CMBO	3	0.27	0.20	3	0.12	0.28	2	0.00	0.12	6	0.06	0.29
KTHA	16	0.09	0.17	15	0.08	0.09	21	-0.10	0.08	21	0.00	0.09
PYL	8	0.03	0.09	9	0.01	0.09	6	0.04	0.12	7	0.04	0.10
AMPL	17	0.14	0.20	17	0.07	0.15	25	0.06	0.12	27	0.06	0.12
CHOS	14	0.00	0.13	14	0.02	0.07	21	-0.10	0.11	20	-0.10	0.10
THERA	15	0.07	0.22	15	0.03	0.16	22	-0.20	0.13	20	-0.20	0.13
NPS	11	0.18	0.16	11	0.10	0.08	13	0.00	0.20	14	0.00	0.21
PRMD	10	0.25	0.28	10	0.24	0.17	15	0.01	0.07	15	0.02	0.06
AOS2	8	-0.10	0.22	8	0.00	0.07	12	-0.10	0.06	14	-0.10	0.06
ATAL	8	-0.10	0.32	7	0.00	0.17	10	0.00	0.10	13	0.00	0.08
VAM	2	0.28	0.23	2	0.18	0.21	7	0.05	0.15	8	0.09	0.17

References

Bocchini G.M., Brüstle A., Becker D., Meier T., van Keken P.E., Ruscic M., Papadopoulos G.A., Rische M., Friederich W., (2018), Tearing segmentation and backstepping of subduction in the Aegean: New insights from seismicity, Tectonophysics, 734–735, pp. 96–118.

Bormann P. and Dewey J.W. (2014). The new IASPEI standards for determining magnitudes from digital data and their relation to classical magnitudes. In: Bormann. P. (Ed.). New Manual of Seismological Observatory Practice 2 (NMSOP-2). Potsdam. Deutsches GeoForschungsZentrum GFZ, pp. 1-44. https://doi.org/10.2312/GFZ.NMSOP-2_IS_3.3.

Di Giacomo D. (2022). Bring Back Systematic Broadband Surface-Wave Magnitude Practice. Seismological Research Letters, Vol 93, no 5, pp. 2413–2417. doi: 10.1785/ 0220220094.

Gutenberg B. (1945). Amplitudes of surface waves and magnitudes of shallow earthquakes. Bulletin of Seismological Society of America, Vol. 35, no. 1, pp. 3–12. doi: 10.1785/BSSA0350010003.

Gutenberg B. (1945a). Amplitudes of P. PP. and S and magnitude of shallow earthquakes. Bulletin of Seismological Society of America, Vol 35, pp. 57–69.

Gutenberg B. (1945b). Magnitude determination of deep-focus earthquakes. Bulletin of Seismological Society of America, Vol. 35, pp. 117–130.

Gutenberg B. and Richter C. F. (1956). Magnitude and energy of earthquakes. Annali di Geofisica, Vol. 9, no 1, pp. 1–15.

Havskov. J. and K. Lieser (2021). Using ISC data. Summ. Bull. International Seismological Centre, January – June 2019, Vol. 56, no I, pp. 30–46. https://doi.org/10.31905/L2IR6ZNA.

Havskov. J. P. Voss and L. Ottemöller (2020). Seismological observatory software: Thirty years of SEISAN. Seismological Research Letters, Vol. 91, pp. 1846-1852.

Helmholtz-Centre Potsdam - GFZ German Research Centre for Geosciences and gempa GmbH. The SeisComP seismological software package. GFZ Data Services. 2008. URL: https://www.seiscomp.de, doi:10.5880/GFZ.2.4.2020.003.

IGME geological maps of Greece 1:50.000, sheets Herakleion, Herson and Myrofyllo.

International Association of Seismology and Physics of the Earth's Interior (IASPEI) (2013). Summary of Magnitude Working Group recommendations on standard procedures for determining earthquake magnitudes rom digital data. available at ftp://ftp.iaspei.org/pub/commissions/CSOI/Summary_WG_recommendations_20130327.pdf .

Kárník V., Kondorskaya N. V., Riznitchenko J. V., Savarensky E. F., Soloviev S. L., Shebalin N. V., Vanek J., and Zátopek A. (1962). Standardization of the earthquake magnitude scale. Stud. Geophys. Geodyn., Vol. 6, pp. 41–48. DOI: 10.1007/BF02590040.

Kennett B.L.N., Engdah E.R.and Buland R. (1995). Constraints on seismic velocities in the Earth from traveltimes. Geophys. J. Int., Vol 122, pp. 108-124.

Kennett B.L.N. and Engdahl E.R. (1991). Travel times for global earthquake location and phase association. Geophysical Journal International, Vol 105, pp. 429-465. DOI:10.17611/DP/9991809.

Kreemer C. and Chamot-Rooke N., 2004. Contemporary kinematics of the southern Aegean and the Mediterranean Ridge, Geophys. J. Int. , Vol. 157, pp. 1377–1392.

Lienert B. and Havskov J. (1995). A Computer Program for Locating Earthquakes Both Locally and Globally. Seismological Research Letters, Vol 66, no5, pp. 26-36. DOI: 10.1785/gssrl.66.5.26.

Lienert B. (1991). Report on modifications made to Hypocenter. Institute of Solid Earth Physics. University of Bergen.

Lienert B., Berg E., Frazer N. (1986). HYPOCENTER: An earthquake location method using centred. scaled and adaptively damped least squares. Bulletin of the Seismological Society of America, Vol 76, no 3, pp.771-783. DOI: 10.1785/BSSA0760030771.

Oliver J. and Murphy L. (1971). WWNSS: Seismology's global network of observing stations. Science, Vol. 174, pp. 254–261. doi: 10.1126/science.174.4006.254.

Peterson J. R. and Hutt C. R. (2014). World-wide standardized seismograph network: A data users guide. U.S. Geol. Surv., Open-File Report. 2014–1218, 74 pp. DOI: 10.3133/ofr20141218.

Peterson J. R. (1993). Observation and modeling of seismic background noise. Open-File report 93-322, USGS, 95pp.

Storchak D.A., J. Schweitzer and P. Bormann (2011). Seismic Phase Names: IASPEI Standard. In: Gupta H.K. (eds) Encyclopedia of Solid Earth Geophysics. Encyclopedia of Earth Sciences Series. Springer. Dordrecht. https://doi.org/10.1007/978-90-481-8702-7_11.

Storchak, D.A., J. Schweitzer, P. Bormann (2003). The IASPEI Standard Seismic Phase List, Seismol. Res. Lett., Vol. 74, no 6, pp. 761-772, https://doi.org/10.1785/gssrl.74.6.761

Vaněk. J., Zapotek A., Karnik V., Kondorskaya N. V., Riznichenko Y. V., Savarensky E. F., Solov'yov S. L. and Shebalin N. V. (1962). Standarizaciya shkaly magnitude. Izvestiya Akad. SSSR. Ser. Geofiz. Vol. 2. pp. 153–158 (with English translation in 1962 by D. G. Frey. published in Izv. Geophys. Ser. (in Russian)).